Archaeological and Anthropological Sciences (2026) 18:10
https://doi.org/10.1007/s12520-025-02379-0

RESEARCH

Pliny's *Creta umbrica* reconsidered: connections with *Terra di nocera* and clay loaves from Umbrian necropoleis

Elisabetta Gliozzo[1] · Pier Lorenzo Fantozzi[2] · Nicoletta Frapiccini[3] · Vayia Xanthopoulou[4] · Ioannis Iliopoulos[5]

Received: 27 May 2025 / Accepted: 26 November 2025 / Published online: 16 December 2025

Abstract
This study investigates the possible correspondence between the modern material known as *Terra di Nocera*, traditionally used in cosmetic and therapeutic applications, and the *creta umbrica* described by Pliny the Elder as a substance employed in textile treatments. The multidisciplinary approach combined mineralogical and geochemical analyses to characterise samples of *Terra di Nocera* (*Scaglia Cinerea* Formation), alongside reference rocks from the *Maiolica* and *Bisciaro* Formations, and unfired clay loaves found in burial contexts at Serravalle di Chienti. The results demonstrate that *Terra di Nocera* is compositionally consistent with parts of the *Scaglia Cinerea* Formation and is characterised by abundant calcite and a clay fraction dominated by illite and smectites—a group of minerals known for their absorptive properties. These properties support its suitability for the textile and therapeutic uses described in ancient sources. The compositional similarity between the archaeological clay loaves and *Scaglia Cinerea* samples suggests a likely shared origin, though post-depositional processes or intentional mixing cannot be excluded. While the identification of *Terra di Nocera* with Pliny's *creta umbrica* remains hypothetical, the analytical evidence lends support to this hypothesis and underscores the cultural and functional relevance of this material from antiquity to the present.

Keywords *Creta umbrica* · *Terra di Nocera* · *Scaglia cinerea* · Nocera Umbra · Fuller's earth

✉ Elisabetta Gliozzo
Elisabetta.gliozzo@unifi.it

Pier Lorenzo Fantozzi
pierlorenzo.fantozzi@unisi.it

Nicoletta Frapiccini
nicoletta.frapiccini@cultura.gov.it

Vayia Xanthopoulou
vxanthopoulou@upatras.gr

Ioannis Iliopoulos
ilios@upatras.gr

1 Department of History, Archaeology, Geography, Fine and Performing Arts, University of Florence, Florence, Italy

2 Department of Physical, Earth and Environmental Sciences, University of Siena, Siena, Italy

3 Ministry of Culture, Ducal Palace of Urbino - Regional Directorate of National Museums of the Marche, State Antiquarium of Numana, Ancona, Italy

4 Laboratory of Electron Microscopy and Microanalysis, School of Natural Sciences, University of Patras, Patra, Greece

5 Department of Geology, University of Patras, Patra, Greece

Introduction

This study explores the intriguing potential link between the *creta umbrica* described by Pliny in the 1st century AD and the contemporary *Terra di Nocera*, sourced from Nocera Umbra (Perugia, Umbria, Italy; Fig. 1), which is renowned today for its therapeutic and cosmetic uses. To circumvent any terminological confusion, it is important to clarify initially that *creta* and *terra* are Latin terms, still used in Italian today, typically translated into English as clay and earth, respectively. However, the classical understanding of *creta* and *terra* may not align precisely with modern interpretations of clay, earth or soil; thus, this paper retains the original denominations to preserve accuracy.

Pliny enumerates six types of *cretae*: *creta cimolia*, *creta thessalica*, *creta sarda*, *creta umbrica*, *saxum* and Tymphaíc gypsum (*Nat*. 35.57.195–198.195), occasionally delineating the properties and applications of each, while in other instances categorising some as variants of *creta Cimolia*.

He specifies two varieties of *creta cimolia*—one white and one purple—utilised by physicians and fullers.

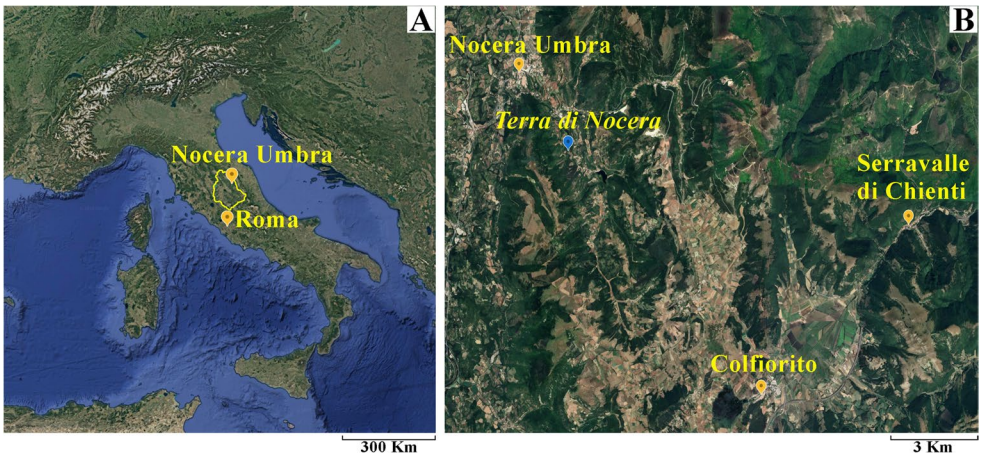

Fig. 1 Satellite map from Google Earth Pro of the principal sites mentioned in the text. Panel **A** delineates the current boundary of the Umbria region. Panel **B** provides an enlargement of the area of interest

Physicians employed these for addressing tumors, treating inflammation and swelling, and curbing excessive perspiration. For the latter purpose, *creta thessalica* was deemed most effective. Although Pliny does not disclose its origin, it is noteworthy that among the localities cited by Theophrastus, the sole site in Thessaly is Perrhaibia, recognized for its natural deposits of Tymphaíc gypsum (Caley and Richards 1956).

In his discourse on the manufacturing of clothing, Pliny identifies three distinct types of *creta cimolia*: *creta sarda*, *creta umbrica* and *saxum*. He notes that the least esteemed among these, *creta sarda*, which was imported from Sardinia, was suitable exclusively for white garments. Contrasting with *creta umbrica*, *saxum* expands upon contact with water—a property that necessitates its purchase by weight rather than by volume, which is the method used for *creta umbrica* (for further discussion on *saxum*, see Rackham 1952; Robertson 1986). The applications of these materials also varied significantly: while *saxum* was employed for whitening garments post-fumigation, *creta umbrica* was reserved for the refurbishment of garments.

Moreover, Pliny provides detailed insights into the specific stages of the process where these materials were utilised. The washing stage employed *creta sarda*; subsequently, the garments were subjected to sulphur fumigation before being treated with *creta cimolia*. In this context, Pliny employs the generic term *creta cimolia*, noted for its ability to soften and rejuvenate colours dulled by fumigation. He further notes that in Greece, Tymphaíc gypsum was used in place of *creta cimolia*.

Regarding supply areas, while the Sardinian origin of *creta sarda* is explicitly stated, Pliny does not confirm that *creta cimolia* originated from Kimolos but instead references a site in Lycia near Bubon[1] where it could be sourced 'in its natural state' (for further reading on Kimolian bentonites from Prassa, Loutra, and Fanara, see Christidis and Scott 1997; Christidis 1998a-b; Christidis 2001).

Undoubtedly, Pliny's text leaves numerous unresolved questions concerning the specific characteristics and origins of each clay, ambiguities that not even comparative analysis with other ancient texts can clarify.

Indeed, even the extensive scholarly debate around the *Lex Metilia fullonibus dicta* mentioned by Pliny offers intriguing insights into the interpretation, context and implications of the law (*e.g.,* Vishnia 1987; Wallinga 1996; Vallocchia 2000; Llamazares Martín 2023), but it does not provide any concrete information about the actual composition of the *cretae*—often derived, directly or indirectly, from the hypotheses proposed by Robertson (1949, 1986). However, he explicitly addresses two critical aspects that intrigue the modern reader: the contemporary applications of these clays in pharmaceutical, cosmetic and clothing industries, and the unique property of certain clays to expand in volume when mixed with water.

Turning to *Terra di Nocera*, this Umbrian white clay is currently promoted for its purported health benefits, including blood and body purification, treatment of gastritis, inflammation, poisoning, arthritic and rheumatic pain, stress and nervous breakdowns. It is also marketed as a cosmetic remedy for acne, rashes, insect bites, eczema and pimples. These claimed uses, however, are derived from promotional material and there is no publicly available clinical evidence confirming their efficacy.

The earliest literary references to Nocera's earth trace back to the 16th century and associate it with local water sources, often referred to as *Acqua Bianca* or *Acqua Angelica*. This association is of particular interest, as it may be seen as part of a broader historical pattern in which the identity and perceived efficacy of medicinal clays were anchored to specific springs or natural settings—often in connection with thermal or healing traditions. In this regard, it is worth noting that Nocera Umbra has long been known for its mineral waters, particularly the Angelica and

[1] Locality also mentioned in *Nat*. 5.28.101-102 where it is inserted in the territory of Cabalia, together with Oenoanda and Balbura.

Flaminia springs (see, also Caldari 2008). However, the available evidence does not allow us to explore this point in further detail.

At that time, local medical practitioners, poets and philosophers were divided over the nature of this local earth. For instance, Bernardino da Spoleto, a physician and physicist from the early 16th century (see Sigismondi 1979, p. 10), categorised it as a *terra sigillata* (understood in this case as a clay used for medical purposes). Bacci (1571) deemed its specific classification—whether Samian, Lemnian or Armenian bole—irrelevant, choosing instead to focus on its practical properties. Meanwhile, Gaspare Ranieri, a poet from the latter half of the 16th century, and Ottaviano Mariani, a physician from Assisi in the same century, both identified it as Lemnian earth (Jacobilli 1653, p. 42; Sigismondi 1979, p. 11).

At the onset of the 17th century, Camilli (1627) reclassified the *Terra di Nocera* as a Samian clay, noting its "bezoartic" (*i.e.* detoxifying, antidotal) properties which aligned it with the medicinal qualities of *Terra di S. Paolo* (from Malta) and *Terra di Mondovì*. Camilli highlighted its refreshing, cleansing, desiccant, anti-inflammatory, healing (for ulcers) and haemostatic effects. However, it was not until Bartolucci (1636, pp. 19–45) that a brief description of the outcrop was provided: "where the said water flows after leaving its source, the stones over which it rapidly passes on its long journey, until it joins the water of the Tupino river, are stained, indeed somewhat imprinted by the said earth" [2]. Subsequent editions, including the expanded second edition of Camilli's treatise (1653) and writings by Dalla Fabra (1712), also noted that the *Terra di Nocera* was extracted near the Bagno di Nocera locality.

Subsequent texts maintain similar information up until 1926, when Bernardino Lotti offered a detailed geological and geochemical analysis of *Terra di Nocera*, also documenting additional names by which it was known:

"Near Nocera, in certain locations within the small valley immediately northwest of the Bagni, the light grey calcareous clayey schists known as 'scaglia cinerea' decompose due to atmospheric conditions, producing a substance locally termed Nocera alkaline earth. Historically purified in water, settled, and dried, this product was once sold in powdered form for the same applications as powdered starch. Currently, it is manufactured into a paste and marketed as 'Angelica paste' in the shape of soap bars. However, this earth acts merely as a mechanical degreaser; it is not genuinely alkaline and bears no connection to the source of Acqua Angelica dei Bagni. Analyses conducted by Engineer G. Aichino in 1911 at the Royal Geological Office Laboratory have demonstrated that it is simply a clayey limestone, as evidenced by the following constituents: loss on ignition (carbonic acid and combined water) 36.84%; silica 11.19%; iron sesquioxide (equivalent to total iron) 1.85%; alumina 3.64%; lime 44.14%; magnesia 0.67%; potash 0.67%; soda 0.95." (adapted from Lotti 1926, pp. 101–102).

A few years later, in 1940, Pinchi published an article in the Italian newspaper *Messaggero* titled 'A Substitute for Soap in the Quarries of Bagni di Nocera'. He described the *Terra di Nocera* as a relatively pure, white smectitic clay, derived from the decay of diorite and commonly referred to as fuller's earth due to its fat-absorbing properties. Pinchi's work also provided the first indication in centuries of this earth's potential use in textile processing: "The ability of this clay to cleanse fabrics from the grease that soils them lies in its absorbent capacity"[3].

During the same period, however, *Terra di Nocera* was also commercialised in the form of stamped soap bars labelled "Terra di Nocera Umbra" (Fig. 2). Unfortunately, we have no information as to whether earlier specimens were also stamped—a detail which, if confirmed, would have evoked the ancient practice of *terrae sigillatae*.

In summary, there are two types of clayey materials: one known as *creta umbrica*, used in the 1st century CE to impart lustre to cloths, and the other known as *Terra di Nocera*, utilized from at least the 16th century to the present for cosmetic and therapeutic purposes but also recognised for its properties as a fuller's earth. These differing functions inevitably entailed variations in the quantities involved—ranging from just a few grams for medicinal use to potentially several kilograms for textile treatment—as well as in the degree of refinement applied to the raw material and, consequently, in transport methods and the distances the product could travel. While it goes without saying that this is a crucial issue to consider, the available evidence does not, at present, allow for a more detailed exploration.

Taken together, however, these considerations highlight the need to view historical uses of clay within a broader context of function, preparation and distribution. In this light, evidence from another site in the region becomes particularly relevant. Archaeological excavations conducted at the necropolis of Colfiorito-Serravalle di Chienti (Bonomi Ponzi 1997; Frapiccini 2022) unearthed several unfired clay masses, often positioned at the feet of the deceased. It is plausible that the specific placement of these clay deposits was symbolic of the significance attributed to the material

[2] "per dove camina dett'Acqua doppo uscita dal suo fonte, le pietre per dove rapidamente passa per lungo viaggio, finchè si congiunge con l'acqua del fiume Tupino, sono imbrattate, anzi impresse alquanto da detta terra".

[3] "La qualità di cui gode quest'argilla di purgare le stoffe dal grasso che le imbratta, riposa nella sua proprietà assorbente."

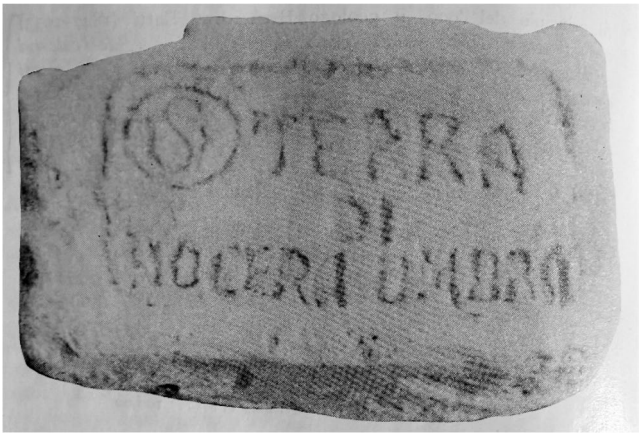

Fig. 2 A mid-20th century stamped soap bar labelled "Terra di Nocera Umbra" from Sigismondi (1979)

itself. Furthermore, Colfiorito is situated less than 20 km southwest of Nocera Umbra, a proximity that has prompted investigations into these clay loaves to ascertain whether they share compositional similarities with those from Nocera Umbra.

As a final observation, it is pertinent to mention that geochemical characterisation of *Terra di Nocera* has seldom been detailed (Table 1), with the mineralogical composition being provided exclusively by Sigismondi (1979) as follows: calcite, montmorillonite, feldspars and quartz. Notably, while the analyses reported by Lotti (1926) and Sigismondi (1979) are broadly comparable, those cited by Pinchi (1940)—on the basis of which he claims that the clay is a product of the decomposition of diorite—are markedly different. However, the article, published in a local newspaper, does not provide any further methodological detail or supporting data that might help clarify this discrepancy.

Given the context presented, the objectives of this study are as follows: (1) to conduct a chemical and mineralogical characterisation of *Terra di Nocera*, assessing its absorbent properties for potential applications in wool processing (*e.g.*, for scouring, fulling and finishing) and for therapeutic and cosmetic uses; (2) to chemically and mineralogically analyse the clay loaves discovered in the necropolis of Colfiorito-Serravalle di Chienti, aiming to elucidate the reasons behind their placement alongside more conventional funerary items within tombs; (3) to carry out a chemical and mineralogical characterisation of *Scaglia Cinerea* taken from the primary quarry of *Terra di Nocera*, with the aim of understanding its properties; and (4) to explore the potential correspondence between Pliny's *creta umbrica* and the more recent *Terra di Nocera* to determine if they are indeed the same material.

Table 1 The chemical composition of the *Terra di Nocera* in literary source. Analytical techniques not specified

Sample	*Terra di Nocera*				Nocera's soap tablet
Reference	Morichini 1807[(1)]	Lotti 1926[(2)]	Pinchi 1940	Sigismondi 1979[(3)]	Sigismondi 1979[(3)]
SiO_2	2 grains	11.19	53	26.90	26.94
TiO_2	-	-	-	0.27	0.18
Al_2O_3	6 grains	3.64	10	6.36	6.29
Fe_2O_3	-	-	-	1.93	1.90
FeO	1 grain	1.85	9.75	0.36	0.43
MnO	-	-	-	0.04	0.03
CaO	-	44.14	0.50	31.44	31.19
MgO	8 grains	0.67	-	1.92	1.95
K_2O	-	0.67	Tr.	0.77	0.76
Na_2O	-	0.95	-	0.41	0.42
P_2O_5	-	-	-	0.12	0.11
$CaCO_3$	71 grains	-	-	-	-
$MgCO_3$[(4)]	-	-	1.25	-	-
L.O.I.	12 grains	36.84	24	29.38	29.41
Total	100 grains	99.95	98.5	99.90	99.61
Ba (ppm)	-	-	-	1470	750
Sr (ppm)	-	-	-	800	800
Zr (ppm)	-	-	-	200	200
Ni (ppm)	-	-	-	150	100
Co (ppm)	-	-	-	2–3	2–3
V (ppm)	-	-	-	1–2	1–2
Cr (ppm)	-	-	-	1–2	1–2
S (ppm)	-	-	-	2–5	2–5
Zn (ppm)	-	-	-	10	10
$CaCO_3$	-	-	-	48.50	49.15
pH	-	-	-	8.4	8.0

[(1)]The "grain" corresponded to the average weight of a grain of wheat. [(2)] Measurements were performed by Prof. G. Aichino in 1911 (Royal Geological Office, Italy). [(3)] Measurements were performed by Prof. G. Dell'Agnola (University of Padova, Italy). [(4)] Reported as "magnesia carbonate"

The territory of the *Terra di Nocera* - geological background

The study area is located in the central-western part of the Italian peninsula and is characterized by a complex landscape, with altitudes reaching up to 2000 m above sea level and extensive alluvial plains. The geological evolution of this region is associated with the thrust-and-fold belt of the Northern Apennines, formed during the Tertiary as a result of the collision between the African and European plates. The main landforms reflect the interplay between fluvial processes and the most recent tectonic uplift phases of the Apennine chain.

Mesozoic and Cenozoic rock formations are exposed in the area under study (Fig. 3; Cita et al. 2005). Among the former, the earliest are from the Jurassic *Calcare*

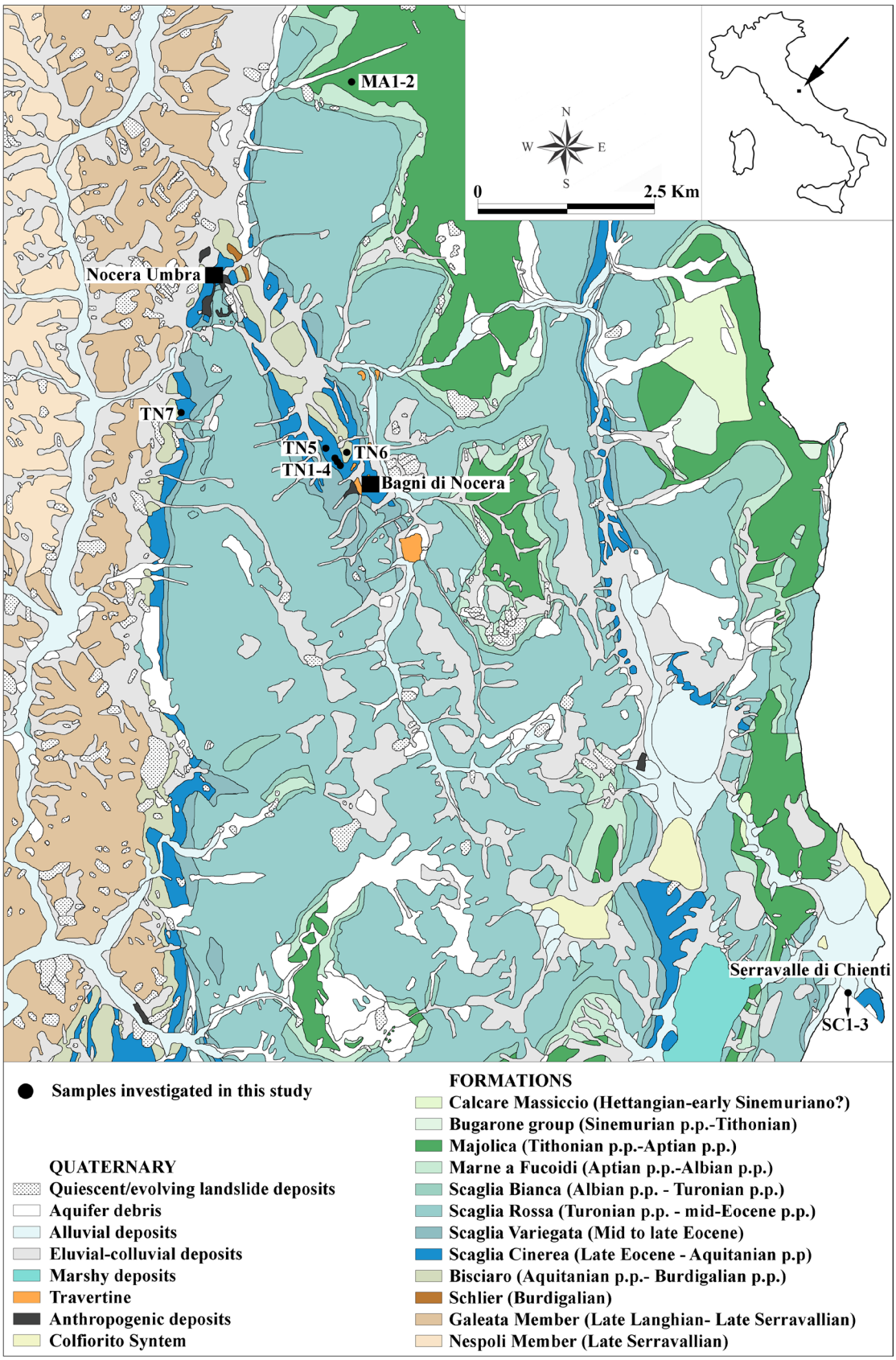

Fig. 3 Geological setting and sampling location. Base map modified based on the vector geological map of the Umbria Region (https://www.regione.umbria.it/paesaggio-urbanistica/cartografia-geologica-informatizzata-vettoriale)

Massiccio Formation, which comprises white to beige and dark grey massive limestones, rich in bioclasts and ooids, and the *Bugarone* Group, which features thick strata of grey to hazelnut micritic limestones, occasionally dolomitised. Proceeding chronologically, the *Maiolica* Formation (sample MA1) consists of micritic limestones distinguished by their conchoidal fracture and predominantly white or very light colouration. These sometimes include nodules of dark flint and are interspersed with greenish pelites (sample MA2). During the early Cretaceous period, the *Marne a Fucoidi* Formation is identified by its marls and marly limestones, notable for bioturbations (Fucoids), and occasionally alternating with bituminous pelites. Spanning the Early and Late Cretaceous periods, the *Scaglia Bianca* Formation derives its name from Lotti (1926). This formation is characterised by white micritic limestones interspersed with numerous bands and layers of dark flint, superimposed upon the Fucoid marls. Bridging the Late Cretaceous and the Middle Eocene—thereby marking the transition from the Mesozoic to the Cenozoic—the *Scaglia Rossa* Formation comprises pink and red micritic limestones. This formation, similar to its predecessor, is named after Lotti (1926). The limestones predominantly alternate with red marls and marly limestones in the upper portion. Where present, the flint is red and appears in bands and nodules. From the Cenozoic period, the *Scaglia Variegata* and *Scaglia Cinerea* Formations are also noted; the former includes polychrome marly limestones alternating with clayey marls, whereas the latter consists of marly limestones and ash-grey or greenish-grey marls (samples TN1a-b/4a-b and TN7a-b).

The latter formation includes the outcrops from which *Terra di Nocera* is extracted (sample TN5a-b). Formed in a pelagic setting, this sequence typically presents a more calcareous basal section transitioning to a predominantly marly upper portion. The boundary with the overlying *Bisciaro* Formation is marked by the emergence of calcareous layers interspersed with black flint and coincides with a volcaniclastic layer known as the 'Raffaello Level' (ranging from 3 to 30 cm in thickness; Coccioni and Montanari 1994). The Umbro-Marche carbonate series culminates with the Miocene *Bisciaro* Formation, which is characterised by siliceous marls and ochre marly limestones interspersed with blackish-grey flint bands and nodules (sample TN6a-b). Intercalations of volcanoclastite create varying degrees of reddened horizons.

In the Burdigalian stage, the *Schlier* Formation forms part of the Umbrian turbiditic series. This formation is differentiated into a basal section composed of silty and grey clayey marls, and an upper section of grey clays and marls, noted for frequent alternations of silty layers. Continuing within the turbiditic series, the *Galeata* and *Nespoli* Members are comprised of pelitic-arenaceous (with frequent calcarenites) and pelitic-arenaceous siliclastic turbidites, respectively.

Lastly, Pleistocene and Holocene sediments encompass landslide, alluvial, eluvial-colluvial and marshy deposits, alongside travertines, anthropic layers and the Colfiorito synthem (Pleistocene deposits that fill intermontane basins).

The clay loaves in the assemblages of the umbrian necropoleis

A vast and rich necropolis has been found at the foot of the Umbrian settlement of Monte Orve (Bonomi 2014), extending across the territories of Colfiorito and Serravalle di Chienti and dated between the 9th and the 3rd century BC (Bonomi 1997; Frapiccini 2022; Pocobelli 2022). Among over 250 burials, nine unfired raw clay 'loaves' were recovered from the assemblages of as many graves, while a tenth loaf was found in a tomb at Terni (Broncoli 2001). A detailed list of the finds and related information drawn from the literature is provided in Table 2.

The tombs containing the loaves include four male and five female burials, all dated between the 6th and the beginning of the 5th century BC. The male tombs belong to high-status individuals, as indicated by grave goods such as weapons, Umbrian and Attic symposium vessels, banqueting utensils and bronze vases. The raw clay loaves were placed beside the feet or near the head of the deceased and, in one case, inside a dish (Bonomi 1997, nn. 3, 6, 176, 177). These placements suggest that the clay loaves may have fulfilled a ritual role within burial

Table 2 Clay loaves in Umbrian necropoleis

	Necropolis	Tomb	Description	Reference
1	Colfiorito	3	Large ovoidal raw clay loaf (Inv. no. 51071)	Bonomi Ponzi 1997
2	Colfiorito	6	Small raw clay loaf (Inv. no. 51141)	Bonomi Ponzi 1997
3	Colfiorito	176	Raw clay loaf (no inventory)	Bonomi Ponzi 1997
4	Colfiorito	177	Small raw clay loaf (Inv. 98891)	Bonomi Ponzi 1997
5	Colfiorito	213	Raw clay loaf (no inventory)	Bonomi Ponzi 1997
6	Colfiorito	248	Small raw clay loaf (Inv. 99348)	Bonomi Ponzi 1997
7	Serravalle	US 170	Small raw clay loaf from a ritual ditch (no inventory)	Frapiccini 2022
8	Serravalle	8	Raw clay loaf (no inventory)	Frapiccini 2022
9	Serravalle	4	Two raw clay loaves (no inventory)	Frapiccini 2022
10	Alterocca di Terni	96/3	Huge clay loaf weighing 22 kg	Broncoli 2001

practices reserved for distinguished individuals, possibly reflecting their therapeutic value.

The grave goods in the female tombs also indicate high social rank, including symposium vessels and jewellery (Bonomi 1997, nos. 213, 248; Frapiccini 2022; nos. 4, 8; Broncoli 2001; no. 96/3). In tomb 4 at Serravalle di Chienti, two clay loaves were discovered: one placed in a bowl, above the feet of the deceased, and the other next to her head, in a so-called niche, *i.e.* a large space obtained by widening the tomb (Fig. 4).

The complete absence of other objects in the niche suggests that it may have been intended for the deposition of perishable goods made of organic materials, which have not been preserved. It cannot be ruled out that these were nonetheless valuable objects, possibly made of wood, leather or even textiles.

This interpretation is tentatively supported by evidence from tomb 213 at Colfiorito, where a spindle whorl was found, and from the Terni tomb, where numerous spools were reportedly embedded in the large clay loaf at the time of excavation (with thanks to Laura Bonomi for this detail). Taken together, these findings may suggest a possible connection between the use of this clay and the weaving activities carried out by the deceased during their lifetime.

The strong ritual significance of the raw clay loaf during the funerary ceremony, even beyond its deposition in the tomb, seems to be further revealed by the presence of this material in other areas of the necropolis. At Serravalle di Chienti, it was clearly identified within a ditch flanking the burials (US 170), together with numerous fragments of intentionally broken pottery—a funerary practice documented in other parts of the necropolis, though previously without evidence of associated clay (Frapiccini 2022, p. 596, Fig. 35.11.A). The pottery fragments found in the ditch are dated between the 7th and 6th centuries BC, indicating that it had been in use for a long time. The deposition of clay in this context likely dates to the 6th century BC, in line with the chronology of the tombs where loaves were recovered.

In conclusion, the data currently available allow us to hypothesise that the clay found in these necropoleis may have served a dual function, textile and therapeutic, reflected in its distinct significance within female and male tombs. Its marked funerary ritual value also seems to be underscored by its deposition in the ditch (US 170), in association with other offerings. This practice appears to have been confined to the 6th to early 5th century BC.

Fig. 4 Serravalle di Chienti (MC), Tomb 4 during the archaeological excavation. The clay loaf in the niche is well recognizable by the lighter color than the burial earth. The second clay loaf was inside the bowl above the feet of the deceased

Materials

In order to address the research questions within the constraints of available evidence, our study focuses on two types of material with clear provenance: the geological source (*Scaglia Cinerea*) and archaeological clay loaves (Table 3). Unfortunately, while no archaeological materials unquestionably identifiable as *creta umbrica* have been found in the northern Umbrian territory, early-modern *Terra di Nocera* products are also not preserved. In addition, modern commercial specimens are subject to undisclosed formulations and provenance, rendering them unsuitable for reliable historical comparison.

Geological sampling primarily focused on the *Scaglia cinerea*, with most samples collected from the outcrop identified as the source area for *Terra di Nocera* (samples TN; Figs. 3 and 5A-C). Within the *Scaglia cinerea* Formation, additional samples (TN1-4 and TN7; Figs. 3 and 5D-E) were collected at various distances from the main outcrop to assess the compositional variability within the area, with TN7 located at the contact between the *Scaglia cinerea* and *Bisciaro* Formations. Given that *Terra di Nocera* is commonly described as a white 'clay'/'earth', the sampling comprised both the in situ rocks (denoted as "TNxa" in Table 3) and the loose materials resulting from its alteration and pedogenesis (denoted as "TNxb" in Table 3). Finally, two more samples from the *Bisciaro* Formation (TN6a-b; Figs. 3 and 5F), cropping out at the base of the hill where *Terra di Nocera* is exploited, and two samples from the *Maiolica* Formation (MA1-2; Figs. 3 and 5G-H) were collected for comparative purposes.

Table 3 Location and description of the investigated samples

Sample	Longitude	Latitude	Formation
TN1a	43°05'24.6"N	12°48'39.9"E	*Scaglia cinerea*
TN1b	"	"	Loose material from the disgregation of TN1a
TN2a	43°05'23.4"N	12°48'41.5"E	*Scaglia cinerea*
TN2b	"	"	Loose material from the disgregation of TN2a
TN3a	43°05'23.4"N	12°48'41.5"E	*Scaglia cinerea*
TN3b	"	"	Loose material from the disgregation of TN3a
TN4a	43°05'22.0"N	12°48'42.6"E	*Scaglia cinerea*
TN4b	"	"	Loose material from the disgregation of TN4a
TN5a	43°05'32.0"N	12°48'30.8"E	*Scaglia cinerea - Terra di Nocera* (rock)
TN5b*	"	"	*Scaglia cinerea - Terra di Nocera* (loose sediment)
TN6a	43°05'32.1"N	12°48'46.4"E	*Bisciaro*
TN6b	"	"	Loose material from the disgregation of TN6a
TN7a	43°05'47.8"N	12°46'57.8"E	*Scaglia cinerea*
TN7b	"	"	Loose material from the disgregation of TN7a
MA1	43°08'20.14"N	12°48'47.23"E	*Maiolica* (active quarry) – white limestone
MA2	"	"	*Maiolica* (active quarry) – greenish pelite level
SC1	43°01'21.4"N	12°53'57.1"E	Serravalle di Chienti necropolis, US 170
SC2	43°01'21.4"N	12°53'57.1"E	Serravalle di Chienti necropolis, tomb 8
SC3	43°01'21.4"N	12°53'57.1"E	Serravalle di Chienti necropolis, tomb 4

*This sample has been sampled twice

With regard to the archaeological samples, the Superintendence of Archaeology, Fine Arts and Landscape of Umbria unfortunately did not authorize EG to analyze the materials from Colfiorito and Terni, primarily due to the destructive nature of the procedures required (10–20 g) and the existence of a previous Mössbauer study conducted on a loaf from Colfiorito (Ortalli et al. 1986). By contrast, the Superintendence of Archaeology, Fine Arts and Landscape for the provinces of Ascoli Piceno, Fermo and Macerata granted permission to analyze materials found in the necropolis of Serravalle di Chienti (NF/22.06.2023). As a result, it was feasible to proceed with the archaeometric analysis of loaves nos. 7–9 listed in Table 2, corresponding to samples SC1-3 in Table 3.

Methods

The samples were analysed through bulk chemical analyses and X-ray powder diffraction.

For bulk chemical analyses, 5 g were ground and submitted to different sample preparation methods and techniques at the Activation Laboratories (Ontario, Canada): (a) lithium metaboratetetraborate fusion on a Thermo Jarrell Ash ENVIRO II inductively coupled plasma optical emission spectrometer (ICP-OES) for determining major elements and Ba, Sr, Y, Zr, and V.

Samples were prepared and analyzed in a batch system, containing a method reagent blank, certified reference material, and 17% replicates. Reagent blanks with and without the lithium borate flux were analyzed, as well as the method reagent blank. Calibration was performed using multiple USGS and CANMET certified reference materials. Two of the standards were used during the analysis for every group of 10 samples; (b) four acid total digestions. A 0.25 g sample aliquot was digested with hydrofluoric, perchloric, hydrochloric, and nitric acids at 200 °C to fuming and was then diluted with aqua regia. The sample solution was spiked with internal standards and introduced into a Perkin Elmer SCIEX ELAN 6000 inductively coupled plasma mass spectrometer (ICP-MS) for determining Cu, Ni, Zn, and Pb. Calibration was performed using USGS and CANMET certified reference materials as above; (c) instrumental neutron activation analysis (INAA) for determining As, Br, Co, Cr, Cs, Hf, Rb, Sb, Sc, La, Ce, Nd, Sm, Eu, Yb, Lu, U, and Th. A 1 g aliquot was encapsulated in a polyethylene vial and irradiated with flux wires and an internal standard (1 for 11 samples) at a thermal neutron flux of $7 \times 1012n \bullet cm-2 \bullet s-1$. After 7-days decay, the samples were counted on a high purity Ge detector. Using the flux wires, the decay-corrected activities were compared with a calibration developed from multiple certified international reference materials. Loss on ignition (LOI) was also determined (1050 °C for 2 h). The Fe^{2+}/Fe^{3+} ratio has not been determined, therefore, $FeO_{(T)}$ stands for total iron. The accuracy was > 5% for Rb and Sr, 10% for Ni, Zr, Ba, La and Ce and 15% for the other elements.

The mineralogical composition of nineteen samples was determined through X-ray powder diffraction analysis (XRPD) employing a Bruker D8 Advance diffractometer, with Ni filtered Cu-Kα radiation, operating at 40 kV/40 mA, equipped with a Bruker LynxEye fast

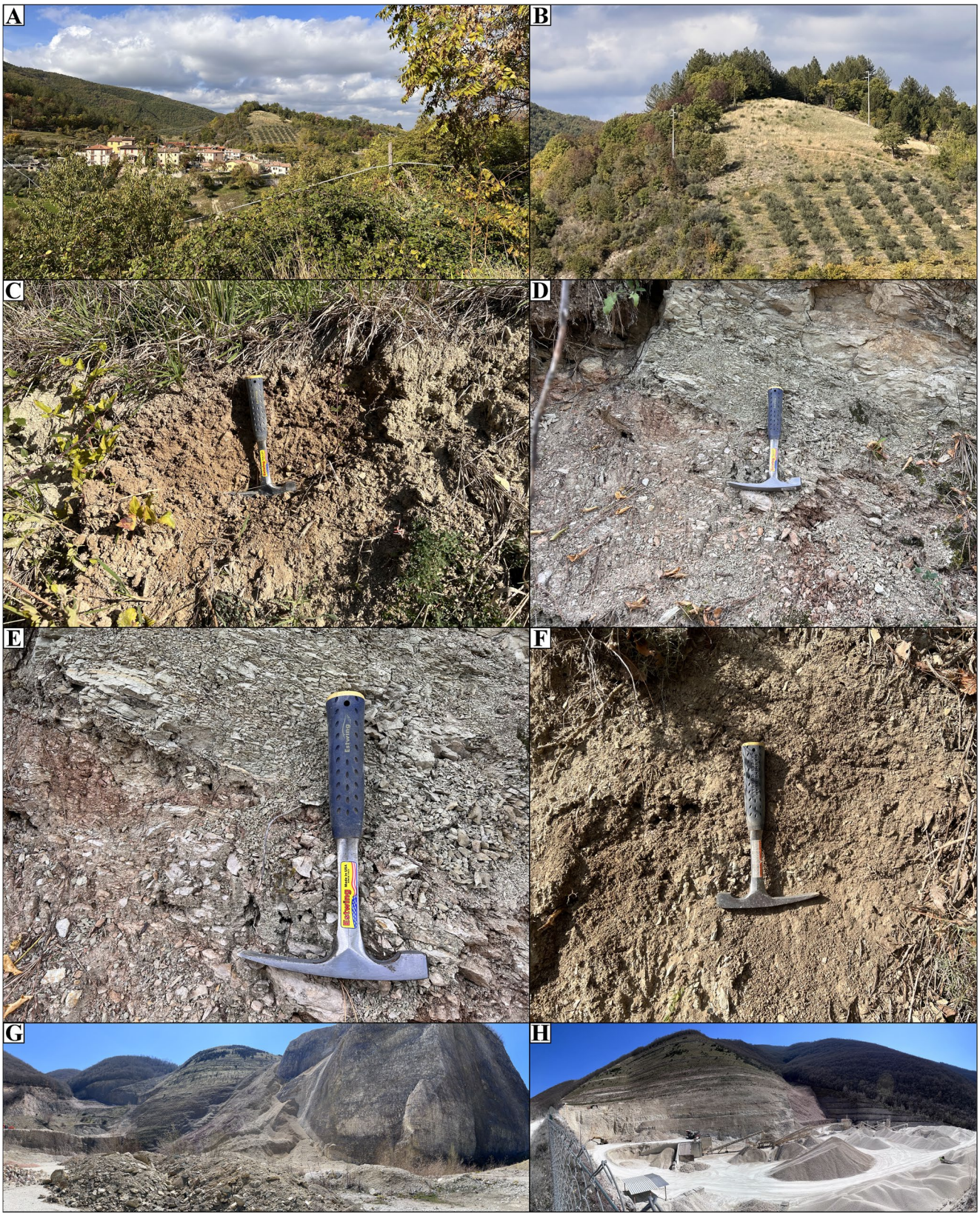

Fig. 5 Sampling sites. **A**-**B**) The hill where *Terra di Nocera* is sourced at varying proximities. **C**) The outcrop of *Terra di Nocera*. **D**-**E**) The *Scaglia cinerea* at the locations where the TN1 samples were collected. **F**) The loose sediments within the *Bisciaro Formation*. **G**-H) Active quarry in the *Maiolica Formation*

detector. The selected samples were treated following a common sequence of pre-treatments (drying, grinding and pulverization), in order to be analysed through X-Ray Diffraction. For the detailed mineralogical characterisation of the samples, two different approaches were followed, considering the bulk mineralogy and the clay minerals determination.

For determining the bulk mineralogy powdered material was accommodated on PVA cylindrical holders with adequate cavities and were scanned from 2 to 70° 2θ, with scanning angle step of 0.015°2θ and a step time of 0.1s.

The clay minerals were evaluated by means of XRPD after the extraction of clay fraction (<2 μm) through sedimentation. The extraction of the clay fraction was carried out using the following procedure (Xanthopoulou and Iliopoulos 2023). After quartering the total amount of the collected material, a small aliquot of the original sample weighing ca. 10 g was gently pulverized in a porcelain mortar using a rubber pestle. Then, 4 g of the pulverized material was placed in a glass tube with a diameter of 2.5 cm and a height of 15 cm with two lines marked on it with a diamond pen; the first line at a height of 2 cm, and the second at 6 cm. The tube was then filled with deionized water up to the first line and some time was allowed to ensure no flocculation occurred. If so, a small amount of Calgon (sodium polyphosphate) was added and the mixture was placed in an ultrasonic bath for 10 min. It was then allowed to settle for 3 h and the material in suspension between the two lines was taken up with a syringe and spread on 3 different smeared glass slides. The slides with the clay fraction were put in a desiccator and left to dry overnight. Three different oriented aggregates were scanned from 2 to 30° 2θ, with scanning angle step of 0.015°2θ and a step time of 0.1s. Qualitative analysis was performed using the DIFFRACplus EVA software ((Bruker-AXS, Madison, WI, USA) based on the ICDD Powder Diffraction File (2006 version).

Quantitative analysis of the bulk material was performed using Rietveld-based refinement with the Topas software. Regarding clay minerals and since these pose challenges for Rietveld refinement due to their poor crystallinity and structural disorder their semi-quantitative determination was instead based on the height of the 001 reflection obtained in the glycolated sample. The peak heights were multiplied by correction factors, taking into consideration the crystallinity of each clay mineral. In the case of samples TN4a and TN6a, the broad reflections of opal-CT and the lack of a relevant structure in TOPAS database hindered reliable refinement. Therefore, for the specific samples only semi-quantitative estimates were obtained by calculating the peak areas of the characteristic reflections.

Results

Geochemistry The results of the bulk chemical analyses (Table 4) highlight the compositional differences that distinguish the various formations considered. The white limestone sampled from the *Maiolica* quarry (MA1) is almost entirely composed of CaO, whereas in the pelitic level sampled from the same quarry (MA2), CaO contents decrease, compensated by an increase in SiO_2, Al_2O_3, Fe_2O_3 and MgO (in decreasing order). The two samples collected from the *Bisciaro* (TN6a-b) are characterized by the lowest CaO contents (28–34 wt%) and the highest SiO_2 contents (52–57 wt%) among all analyzed samples. The samples collected from the *Scaglia Cinerea* (TN1a-b, TN5a-b, TN7a-b) form a relatively heterogeneous group, primarily characterized by variable SiO_2 contents ranging from 13 to 33 wt% (average 23 wt%, s.d. 5), Al_2O_3 from 4 to 11 wt% (average 8 wt%, s.d. 2), Fe_2O_3 from 2 to 5 wt% (average 3 wt%, s.d. 1), MgO from 1 to 2 wt% (average 1 wt%, s.d. 0.3) and CaO from 47 to 78 wt% (average 62 wt%, s.d. 9). In particular, the *Terra di Nocera* samples (TN5a-b) do not show substantial differences compared to the rest of the *Scaglia Cinerea* group, except that sample TN5b exhibits the highest CaO content. Among the archaeological samples, SC3 is compositionally compatible with the *Scaglia Cinerea* group, while SC1 and SC2 display higher CaO contents and lower SiO_2, Al_2O_3 and MgO contents. Volatiles, measured as loss on ignition (LOI), are consistently high across all samples, ranging from 9 to 43 wt% with an average of 34 wt% (s.d. 8), except for sample TN4a, which shows the lowest value.

Based on the classification proposed by Correns (1939, 1949), the samples can be grouped as clayey marl (25–35 wt% $CaCO_3$; TN4a), marl (35–65 wt% $CaCO_3$; TN4b, TN5b and TN6a-b), calcareous marl (65–75 wt% $CaCO_3$; MA2, TN1a-b, TN2b, TN3a-b, TN5a and TN7a-b), marly limestone (75–85 wt% $CaCO_3$; TN2a and SC3) and slightly marly limestone (85–95 wt% $CaCO_3$; MA1, SC1 and SC2).

The geochemical variability of the samples can also be effectively represented through a ternary plot following Brumsack (1989), which employs CaO as an indicator of carbonate content, SiO_2 as a proxy for quartz and Al_2O_3 to reflect the presence of aluminosilicate phases, primarily clay minerals (Fig. 6A).

The distribution of the samples aligns along a trend from the carbonate-rich corner toward the average shale composition, within the aluminosilicate field. The samples from the *Maiolica* quarry and some of the *Scaglia Cinerea* and archaeological samples cluster near the carbonate corner, reflecting their higher carbonate content.

In contrast, the *Bisciaro* samples are distinctly shifted toward the quartz-rich field, consistent with their lower CaO and higher SiO_2 and Al_2O_3 contents. Notably, sample TN4a

Table 4 Bulk Chemistry. Major elements contents were normalised to 100% (without LOI values). All values recorded for Mo, Ag, In, W, and Bi were below detection limits and have consequently not been included in the table

	SiO_2	Al_2O_3	$FeO_{(T)}$	MnO	MgO	CaO	Na_2O	K_2O	TiO_2	P_2O_5	LOI	Sc	Be	V	Ba	Sr	Y
Det.lim. (%-ppm)	0.01	0.01	0.01	0.005	0.01	0.01	0.01	0.01	0.001	0.01	-	1	1	5	2	2	1
TN1a	19.92	6.47	2.54	0.20	1.11	67.88	0.16	1.29	0.27	0.16	36.41	4	<1	35	74	931	14
TN1b	20.80	6.84	2.69	0.19	1.17	66.35	0.14	1.37	0.29	0.16	36.19	4	<1	39	78	928	14
TN2a	13.43	4.42	1.64	0.28	0.82	78.19	0.12	0.80	0.18	0.13	38.78	3	<1	29	330	954	11
TN2b	19.33	6.48	2.46	0.27	1.10	68.50	0.13	1.26	0.28	0.18	37.07	4	<1	43	161	855	14
TN3a	20.71	6.78	2.37	0.19	1.17	66.86	0.13	1.30	0.30	0.18	36.22	4	<1	35	94	864	13
TN3b	24.61	8.04	2.93	0.18	1.34	60.61	0.14	1.61	0.37	0.17	35.11	5	1	44	131	788	15
TN4a	26.10	7.40	3.41	0.19	1.92	56.76	1.34	2.13	0.42	0.32	38.73	12	2	43	143	808	15
TN4b	30.44	10.06	4.03	0.23	1.64	50.94	0.25	1.81	0.43	0.18	33.59	7	1	58	316	811	18
TN5a	26.20	8.75	3.61	0.31	1.41	57.38	0.20	1.60	0.39	0.15	34.11	6	1	71	196	982	16
TN5b	33.09	10.90	4.58	0.22	1.73	46.65	0.21	1.95	0.51	0.17	32.42	8	1	67	355	831	17
TN6a	57.19	4.55	1.57	0.04	0.67	34.25	0.34	1.10	0.19	0.10	24.40	4	<1	37	909	710	15
TN6b	52.29	11.39	3.97	0.07	1.78	27.60	0.51	1.76	0.44	0.18	27.34	8	2	48	1713	544	26
TN7a	20.22	6.43	2.62	0.17	1.16	67.46	0.22	1.29	0.28	0.14	36.03	4	<1	34	1710	1008	13
TN7b	23.62	7.52	2.94	0.15	1.34	62.12	0.27	1.56	0.34	0.16	35.13	5	<1	46	1218	967	14
MA1	3.41	0.61	0.30	0.06	0.71	94.65	0.05	0.12	0.02	0.05	42.69	<1	<1	<5	13	238	8
MA2	24.44	8.05	3.07	0.20	1.32	60.65	0.22	1.56	0.33	0.16	34.54	5	<1	51	117	878	12
SC1	8.54	2.67	0.94	0.19	0.68	86.30	0.09	0.42	0.10	0.09	40.78	2	<1	16	42	468	12
SC2	8.50	2.74	1.02	0.17	0.66	86.18	0.10	0.43	0.10	0.09	40.94	2	<1	15	39	530	13
SC3	17.93	2.66	1.15	0.15	0.68	76.76	0.08	0.38	0.10	0.10	38.59	2	<1	13	46	302	16
	Zr	Cr	Co	Ni	Cu	Zn	Ga	Ge	As	Rb	Nb	Sn	Sb	Cs	La	Ce	Pr
Det.lim. (ppm)	2	20	1	20	10	30	1	1	5	2	1	1	0.5	0.5	0.1	0.1	0.05
TN1a	32	40	13	40	30	40	6	<1	<5	37	4	1	<0.5	2.4	14.9	22.9	2.95
TN1b	37	40	11	50	30	40	6	<1	<5	38	4	1	<0.5	2.4	15.0	23.8	3.11
TN2a	22	20	3	30	20	<30	4	<1	<5	21	2	<1	<0.5	1.4	11.0	15.5	2.17
TN2b	34	30	18	50	30	50	6	<1	<5	35	4	1	<0.5	2.3	15.2	22.7	2.88
TN3a	43	30	3	40	30	40	6	<1	<5	33	4	1	<0.5	2.1	13.8	21.7	2.84
TN3b	51	40	10	50	30	50	7	<1	<5	42	5	1	<0.5	2.7	15.9	25.9	3.32
TN4a	59	60	14	80	40	70	10	1	<5	49	9	1	0.5	2.6	21.4	37.9	4.58
TN4b	65	60	11	90	40	60	9	<1	<5	52	7	1	0.5	3.5	20.0	36.1	4.30
TN5a	53	60	44	100	50	60	8	<1	7	47	6	1	0.6	3.3	18.8	34.8	4.17
TN5b	74	70	33	100	40	80	11	<1	8	60	8	1	0.7	4.2	21.2	40.4	4.53
TN6a	38	30	<1	20	30	60	6	<1	<5	38	3	1	<0.5	2.1	14.4	17.6	2.80
TN6b	109	30	7	40	40	80	11	<1	<5	60	7	2	<0.5	4.1	21.2	39.0	4.77
TN7a	38	40	<1	40	20	40	6	<1	<5	36	4	1	<0.5	2.3	13.9	21.9	2.88
TN7b	44	50	6	50	40	50	7	<1	6	43	5	1	<0.5	2.9	15.1	24.7	3.17
MA1	4	<20	<1	<20	10	<30	1	<1	<5	2	<1	<1	<0.5	<0.5	5.8	3.2	0.91
MA2	41	40	11	50	20	50	7	<1	14	42	4	1	<0.5	2.8	13.3	23.1	2.75
SC1	13	<20	<1	<20	10	<30	2	<1	<5	11	1	<1	<0.5	0.8	16.2	9.7	2.42

Table 4 (continued)

	SiO_2	Al_2O_3	$FeO_{(T)}$	MnO	MgO	CaO	Na_2O	K_2O	TiO_2	P_2O_5	LOI	Sc	Be	V	Ba	Sr	Y
SC2	12	<20	<1	<20	10	<30	2	<1	<5	11	1	<1	<0.5	0.7	16.6	9.2	2.48
SC3	15	<20	<1	<20	10	<30	2	<1	<5	12	1	<1	<0.5	1.0	13.8	10.1	2.29
	Nd	Sm	Eu	Gd	Tb	Dy	Ho	Er	Tm	Yb	Lu	Hf	Ta	Tl	Pb	Th	U
Det.lim. (ppm)	0.1	0.1	0.05	0.1	0.1	0.1	0.1	0.1	0.05	0.1	0.01	0.2	0.1	0.1	5	0.1	0.1
TN1a	12.3	2.4	0.55	2.2	0.3	2	0.4	1.3	0.18	1.1	0.17	0.7	0.3	0.2	7	3.0	0.5
TN1b	12.8	2.5	0.54	2.1	0.3	2.1	0.4	1.2	0.17	1.1	0.18	0.9	0.2	0.2	7	3.1	0.6
TN2a	8.8	1.7	0.4	1.7	0.3	1.5	0.3	1	0.15	1	0.15	0.5	0.1	0.1	6	1.8	0.4
TN2b	12.0	2.3	0.51	2.1	0.4	2	0.4	1.3	0.17	1.1	0.18	0.9	0.2	0.2	8	2.9	0.5
TN3a	11.3	2.4	0.48	2.0	0.3	1.8	0.4	1.2	0.17	1.1	0.18	0.9	0.3	0.2	8	2.9	0.5
TN3b	13.6	2.5	0.6	2.4	0.4	2.1	0.4	1.3	0.19	1.3	0.19	1.2	0.3	0.3	8	3.5	0.6
TN4a	16.6	4.1	0.81	2.9	0.6	2.9	0.7	1.8	0.34	1.8	0.27	1.8	0.5	0.3	10	5.1	1.1
TN4b	17.1	3.7	0.74	2.8	0.5	2.7	0.6	1.7	0.25	1.7	0.26	1.6	0.5	0.3	10	4.9	1.0
TN5a	17.0	3.5	0.76	2.9	0.5	2.7	0.5	1.5	0.23	1.6	0.25	1.3	0.3	0.2	13	4.1	1.0
TN5b	18.6	3.7	0.76	3.1	0.5	2.7	0.6	1.7	0.26	1.8	0.27	1.9	0.5	0.3	13	5.4	1.1
TN6a	11.4	2.1	0.48	2.2	0.4	2.2	0.5	1.3	0.19	1.3	0.21	0.9	0.2	0.3	6	2.7	2.9
TN6b	20.0	4.2	0.84	3.8	0.6	3.8	0.8	2.4	0.36	2.4	0.39	2.8	0.5	0.3	13	6.5	2.3
TN7a	11.8	2.3	0.52	2.1	0.3	1.9	0.4	1.2	0.17	1.1	0.17	0.9	0.2	0.2	6	2.8	0.6
TN7b	13.1	2.5	0.57	2.3	0.4	2.0	0.4	1.2	0.18	1.2	0.20	1.1	0.3	0.3	8	3.5	0.7
MA1	4.3	0.9	0.23	1.1	0.2	0.9	0.2	0.6	0.09	0.5	0.08	<0.2	<0.1	<0.1	<5	0.2	0.4
MA2	11.6	2.3	0.49	2.0	0.3	1.8	0.4	1.1	0.15	1.0	0.17	1.1	0.3	0.2	10	3.5	0.8
SC1	10.1	1.7	0.41	1.8	0.3	1.5	0.3	0.9	0.13	0.8	0.13	0.2	<0.1	<0.1	<5	1.1	0.2
SC2	10.3	1.8	0.41	2.0	0.3	1.6	0.3	1.0	0.13	0.9	0.13	0.2	<0.1	<0.1	<5	1.0	0.2
SC3	9.6	1.8	0.42	1.9	0.3	1.7	0.4	1.2	0.16	1.0	0.16	0.4	<0.1	<0.1	<5	1.2	0.2

plots near the apex representing clay minerals, confirming its distinctive composition with elevated aluminosilicate content and lower carbonate. The *Terra di Nocera* samples (blue) and most of the *Scaglia Cinerea* samples occupy an intermediate position, indicating variable but significant carbonate contributions with minor enrichment in clay minerals and silica.

The discrimination diagram of Roser and Korsch (1988) provides additional insight into the provenance of the analyzed samples (Fig. 6B). Most of the samples plot in the field indicative of intermediate igneous provenance, suggesting a dominant contribution from a continental source area. A slight shift is observed for sample TN4a and the *Bisciaro* samples, consistent with their distinctive geochemical signature already highlighted in the ternary diagram. Sample MA1 is presented for completeness; however, given its nature as a carbonate-rich *Maiolica*, its classification within the quartzose sedimentary provenance field based on the discrimination diagram is not reliable, as the result is likely compromised by the significant carbonate content.

The binary diagrams (Fig. 6C–K) illustrate the relationships between Al_2O_3 and the major oxides, as well as Sc. Overall, most elements display strong to very strong linear correlations with Al_2O_3. SiO_2 (Fig. 6C) shows a moderately positive correlation ($R^2 = 0.62$) but with noticeable scatter, especially due to samples such as TN4a and some archaeological specimens (*e.g.*, MA1 and SC3). Conversely, Fe_2O_3, MgO, K_2O, TiO_2, P_2O_5, and Sc (Fig. 6D, E, H, I, J and K) exhibit excellent linear trends with Al_2O_3 (R^2 ranging from 0.91 to 0.99). CaO (Fig. 6F) is negatively correlated with Al_2O_3 ($R^2 = 0.78$), reflecting the dilution effect exerted by the carbonate fraction on the aluminosilicate components. The scatter shown by *Bisciaro* samples is consistent with their lower carbonate content and higher siliciclastic input. Na_2O (Fig. 6G) also shows a good positive correlation ($R^2 = 0.71$), despite a slightly higher variability compared to the other oxides.

With regard to minor and trace elements, Sr and Ba are the most abundant. The primitive mantle (PM)–normalized and upper continental crust (UCC)–normalized trace element patterns are shown in Fig. 7. Trace elements are generally depleted relative to the PM, except for Zr and Hf in the archaeological samples and the limestone MA1. Compared to the UCC, all samples show depletion for most elements, except for Ba and Sr, which are relatively enriched.

The PM-normalized diagrams (Fig. 7A-B) show that the analyzed samples are mainly enriched in large-ion lithophile elements (LILE; Rb, Cs, Sr, Ba) and REEs, while the high field-strength elements (HFSE; Nb, Ta, Zr, and Hf) are near unity or depleted. All samples follow a very similar pattern, although the archaeological samples (together with sample MA1) are consistently depleted compared to the others. The only element showing a different behavior is Pb, which exhibits a weak positive anomaly in the *Scaglia Cinerea* and *Terra di Nocera* samples but a negative anomaly in the archaeological ones. Notably, all samples display negative Ce and Eu anomalies and positive anomalies of Pr and, to a lesser extent, Gd.

The UCC-normalized diagrams (Fig. 7C–D) similarly show that the samples follow comparable, largely depleted patterns, except for Ba in almost all samples and Sr in the *Bisciaro* samples and three *Scaglia Cinerea* samples (TN2a and TN7a–b). The archaeological samples follow a very similar pattern among themselves and are well comparable with the remaining *Scaglia Cinerea* and *Terra di Nocera* samples. Notably, Zr and Hf exhibit negative anomalies and a pronounced negative Ce anomaly is observed across all samples, while the Eu anomaly is weaker but still evident.

Mineralogy The mineralogical phases identified in the studied samples are quartz, calcite, dolomite, opal-CT and clay minerals (Table 5). The *d*-spacings of the main reflections used for mineral identification are the following:

- Quartz (SiO_2) reflections (PDF ID: 00–046−1045): 3.34 Å, 4.26 Å, 2.46 Å, 2.28 Å, 2.24 Å, 2.13 Å, 1.81 Å.
- Calcite ($CaCO_3$) reflections (PDF ID: 00–005−0586): 3.04 Å, 3.86 Å, 2.49 Å, 2.28 Å, 2.10 Å.
- Dolomite [$CaMg(CO_3)_2$] reflections (PDF ID: 01–079−1345): 2.89 Å, 2.67 Å. 2.41 Å, 2.19 Å, 2.02 Å.
- Opal-CT (SiO_2 H_2O) reflections: ~ 4.07 Å (Guthrie et al. 1995).
- Baryte ($BaSO_4$) reflections (PDF ID: 01–076−0214): 5.57 Å, 4.35 Å, 3.57 Å.

The main reflections used for clay minerals identification are described below:

a) illite: it was identified by the main reflection $d(001) = 10$ Å and those at $d = 4.97$ Å, 4.48 Å and 3.3 Å (the latter overlapping an intense quartz peak).
b) smectite: it was identified after ethylene-glycol treatment at $d = 16.6$ Å, collapsing to $d = 10$ Å after heating treatment.
c) kaolinite: it was identified by reflections at $d(001) = 7.16$ Å and at $d(002) = 3.58$ Å, compared with chlorite reflections at $d(002)$ and $d(004)$.

Random mixed layers were also detected. The nomenclature follows Thorez (1976):

a) chlorite-smectite (14c-14s). The main reflection of the interstratified structure (14c-14s) occurs at about 14 Å in the air-dried state. It swells to about 15.6 Å

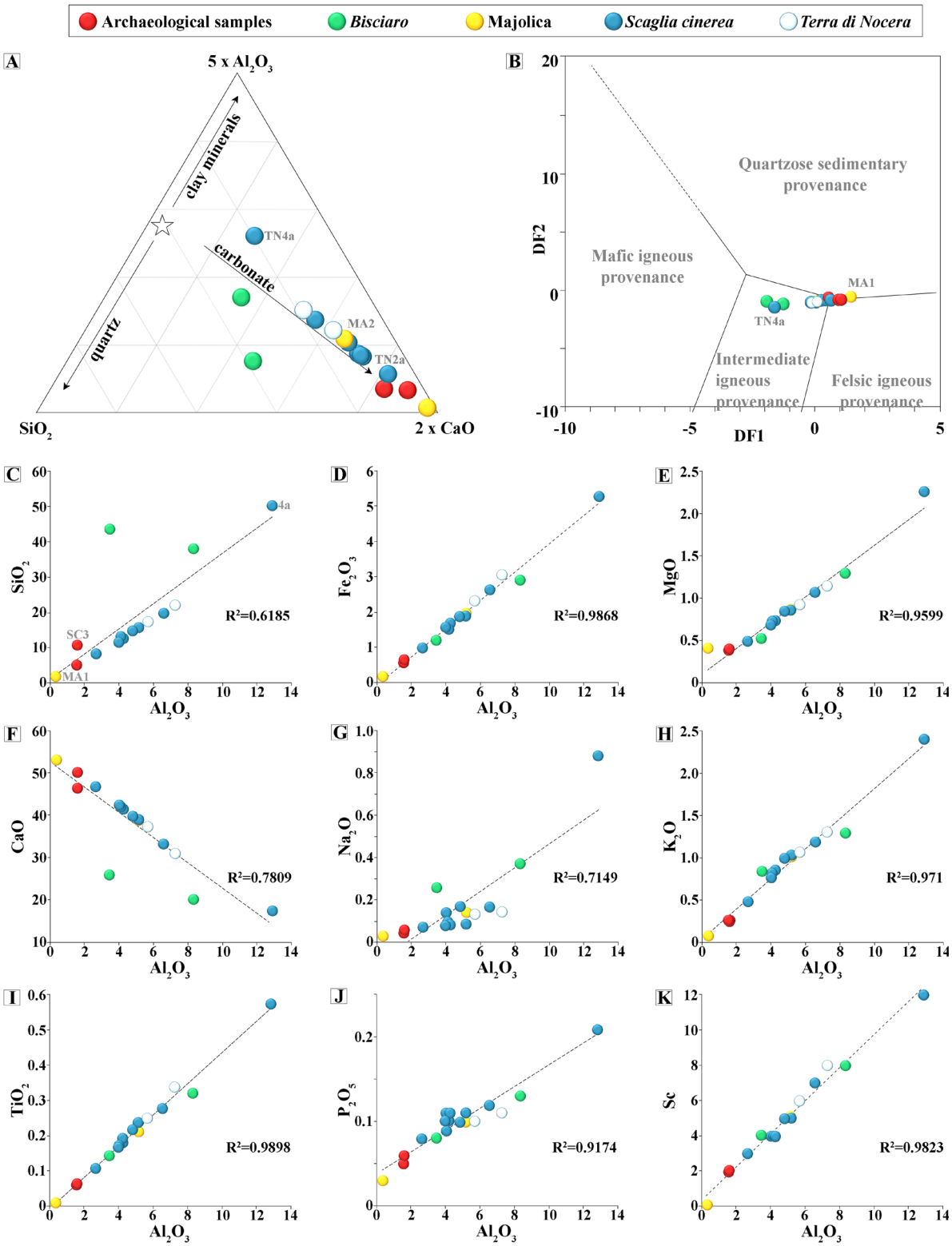

Fig. 6 Geochemical composition of the investigated samples. (**A**) Ternary diagram $5\times Al_2O_3$–SiO_2–$2\times CaO$ (modified after Brumsack 1989) including the average shale composition from Wedepohl (1971). (**B**) Discriminant function plot (DF1 *vs.* DF2) following Roser and Korsch (1988), using the ratio of major oxides to Al_2O_3 to generate the DF1 and DF2 ($DF1 = 30.638\ TiO_2/Al_2O_3 - 12.541\ Fe_2O_3(t)/Al_2O_3 + 7.329\ MgO/Al_2O_3 + 12.031\ Na_2O/Al_2O_3 + 35.402\ K_2O/Al_2O_3 - 6.382$; $DF2 = 56.500\ TiO_2/Al_2O_3 - 10.879\ Fe_2O_3(t)/Al_2O_3 + 30.875\ MgO/Al_2O_3 - 5.404\ Na_2O/Al_2O_3 + 11.112\ K_2O/Al_2O_3 - 3.89$). (**C**–**K**) Binary diagrams illustrating the linear correlation between Al_2O_3 and the other major oxides, as well as Sc. All values are expressed in wt%, except for Sc in diagram (K), which is in ppm. Note that sample MA2 is often overlapped by *Scaglia Cinerea* samples and samples SC1 and SC2 also frequently overlap. The R^2 values are calculated considering all samples

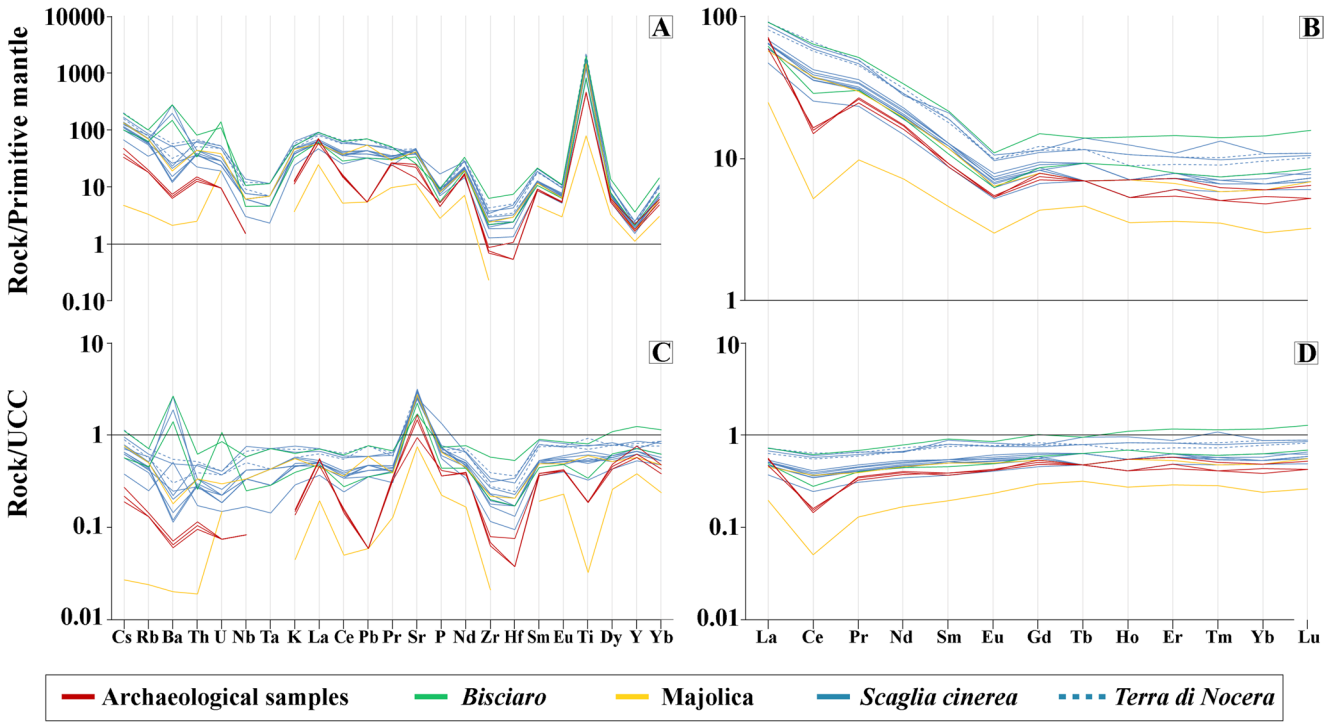

Fig. 7 Multi-element (**A**, **C**) and rare earth element (REE) (**B**, **D**) spider diagrams for all analyzed samples. Diagrams (**A**) and (**B**) are normalized to the primitive mantle composition of Sun & McDonough (1989), while diagrams (**C**) and (Geochemistry) are normalized to the upper continental crust (UCC) values of Rudnick & Gao (2014)

upon glycolation and collapses to ~12 Å after heating treatment. The main peak of the interstratified structure (14c-14v) occurs at about 14 Å (natural and glycolated sample). After heating treatment this peak occurs at about 12.3 Å. In some cases, the peak at d=14 Å is replaced by a broad diffraction band between 13.2 and 12.3 Å.

b) illite-smectite (10–14 s). The main reflection of the interstratified structure (10–14 s) exhibits a broad, asymmetric reflection towards the high angle side, at about 12.6 Å, which is shifted to ~13.6 Å in some samples or is replaced by a single peak at about 17.6 Å (glycolated sample), though this collapses to 10 Å on heating.

c) mica-vermiculite (10-14v). The principal peak of the interstratified structure (10-14v) is situated at about 13 Å, without any change after glycolation and it collapses at about 10Å after heating.

The results of the XRPD analysis of the bulk samples indicate that all samples are dominated by high amounts of calcite. Based on their mineralogical assemblages, the samples can be grouped into three compositional categories (Fig. 8). The first group, consisting of four samples (MA1, SC1, SC3 and TN3a), is characterized by the presence of calcite and minor quantities of quartz. Sample TN3a additionally contains trace of kaolinite and baryte. The second group, represented by thirteen samples (TN1a-b, TN2a-b, TN3b, TN4b, TN5a-b, TN6b, TN7a-b, MA2 and SC2), is composed of calcite, quartz and clay minerals, with minor amounts of dolomite and illite. The third group includes two samples (TN4a and TN6a) and is characterized by the presence of calcite, quartz, fewer quantities of clay minerals and opal-CT, and minor dolomite and illite.

The analysis of the clay fraction (<2 µm, oriented samples) (Table 5; Fig. 9) reveals that smectite and illite are the dominant phases, while kaolinite and mixed-layer minerals, including chlorite/smectite and mica/vermiculite, occur less frequently. Further distinctions can be drawn based on the relative proportions of clay minerals. Before proceeding, it is worth noting that the clay fraction of the limestone sample MA1 consists solely of illite, with no kaolinite, smectite, or mixed-layer phases identified. In contrast, the clay fraction of sample TN2b comprises kaolinite and illite, while the mixed-layer phases appear to be exclusively represented by mica/vermiculite (Fig. 9A). Among the remaining samples, three subgroups can be distinguished. The first subgroup (Fig. 9B) includes four *Scaglia Cinerea* samples (TN1a, TN3b, TN4a and TN5a), where illite and smectite represent the main clay phases, accompanied by minor amounts of kaolinite or

Table 5 Mineralogical composition (wt%) of the bulk sample and the <2 μm fraction as determined by XRPD analysis on powdered and oriented samples, respectively (tr: traces; -: below detection limits)

		Bulk sample					<0.002 mm fraction			
		Calcite	Quartz	Opal-CT	Dolomite	Clay Minerals	Illite	Kaolinite	Smectite	Mixed layers
Maiolica	MA1	93	2	-	tr	5	100	-	-	-
Scaglia cinerea	TN2b	90	4	-	tr	5	12.7	3.7	-	83.6
Scaglia cinerea	TN4a	30	19	19	tr	32	32.4	-	67.6	-
Scaglia cinerea	TN3b	89	4	-	tr	7	16.8	4.2	79.0	-
Scaglia cinerea	TN5a	84	6	-	tr	10	22.1	5.9	-	72.0
Scaglia cinerea	TN1a	87	5		tr	8	7.9	1.7	30.0	60.4
Scaglia cinerea	TN1b	85	6	-	tr	10	15.7	2.6	81.8	-
Scaglia cinerea	TN7a	91	5	-	tr	4	14.1	2.7	36.8	46.4
Scaglia cinerea	TN7b	86	6	-	tr	8	13.8	0.0	32.0	54.3
Bisciaro	TN6a	38	8	12	tr	42	15.8	0.0	35.6	48.6
Archaeological	SC1	99	1		tr	-	16.1	0.0	32.8	51.1
Scaglia cinerea	TN2a	95	3	-	tr	2	11.9	2.3	85.8	-
Scaglia cinerea	TN3a	99	1	-	tr	-	11.9	2.4	36.0	49.8
Scaglia cinerea	TN4b	72	8	-	tr	20	9.7	3.7	44.5	42.1
Scaglia cinerea	TN5b	71	8	-	tr	22	20.8	7.9	71.4	-
Bisciaro	TN6b	29	5	-	tr	66	10.3	0.0	89.7	-
Maiolica	MA2	82	6	-	tr	12	9.9	1.9	34.0	54.1
Archaeological	SC3	93	8	-	-	-	5.6	1.1	33.1	60.1

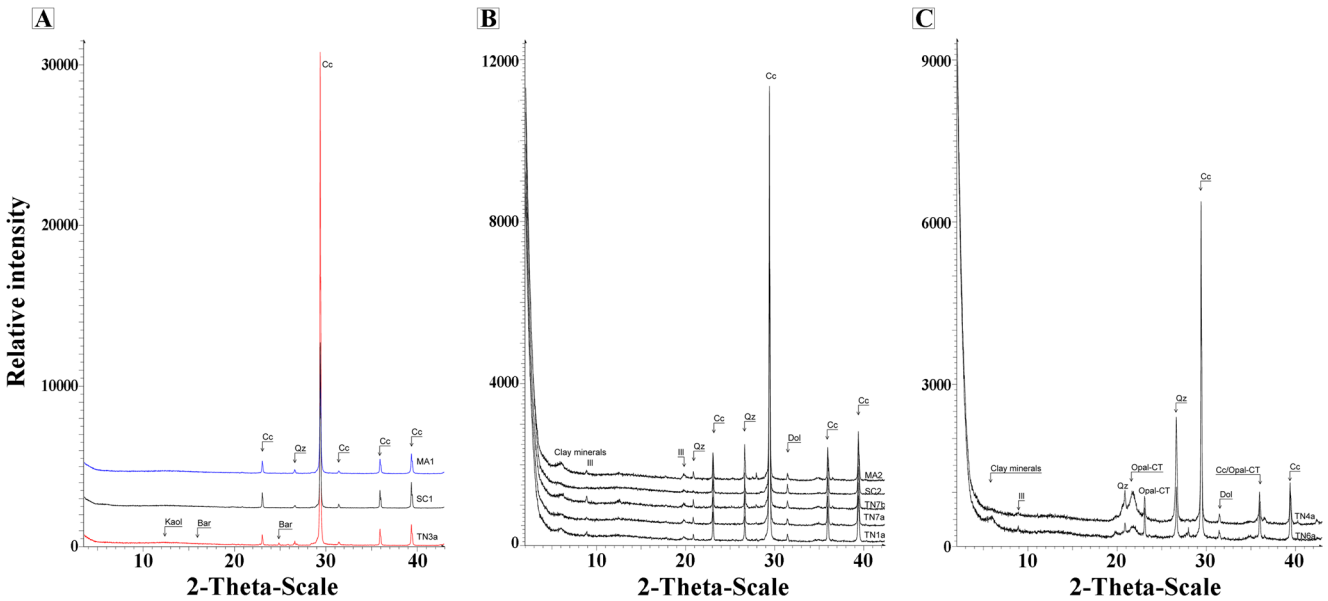

Fig. 8 Stacked XRPD patterns of the first (**A**), second (**B**), and third (**C**) groups as defined by the bulk sample analysis. Mineral abbreviations: Qz = quartz; Cc = calcite; Dol = dolomite; Ill = illite; Bar = baryte

chlorite or mixed-layer chlorite/smectite. The second subgroup (Fig. 9C) consists of three *Scaglia Cinerea* samples (TN1b, TN5b, TN7a-b), one *Bisciaro* sample (TN6a) and two archaeological samples (SC1 and SC3), where illite and smectite are present in amounts almost similar to those of mixed-layer illite/smectite and kaolinite occurs only sporadically. The third subgroup (Fig. 9D) comprises three *Scaglia Cinerea* samples (TN2a, TN3a, TN4b), one *Bisciaro* sample (TN6b) and one *Maiolica* sample (MA2) where the main clay phases are illite, smectite and mixed-layer illite/smectite, associated with minor kaolinite and, in two cases, mixed-layer chlorite/smectite. Clay fraction analysis was not performed for sample SC2 due to the very small amount of material available.

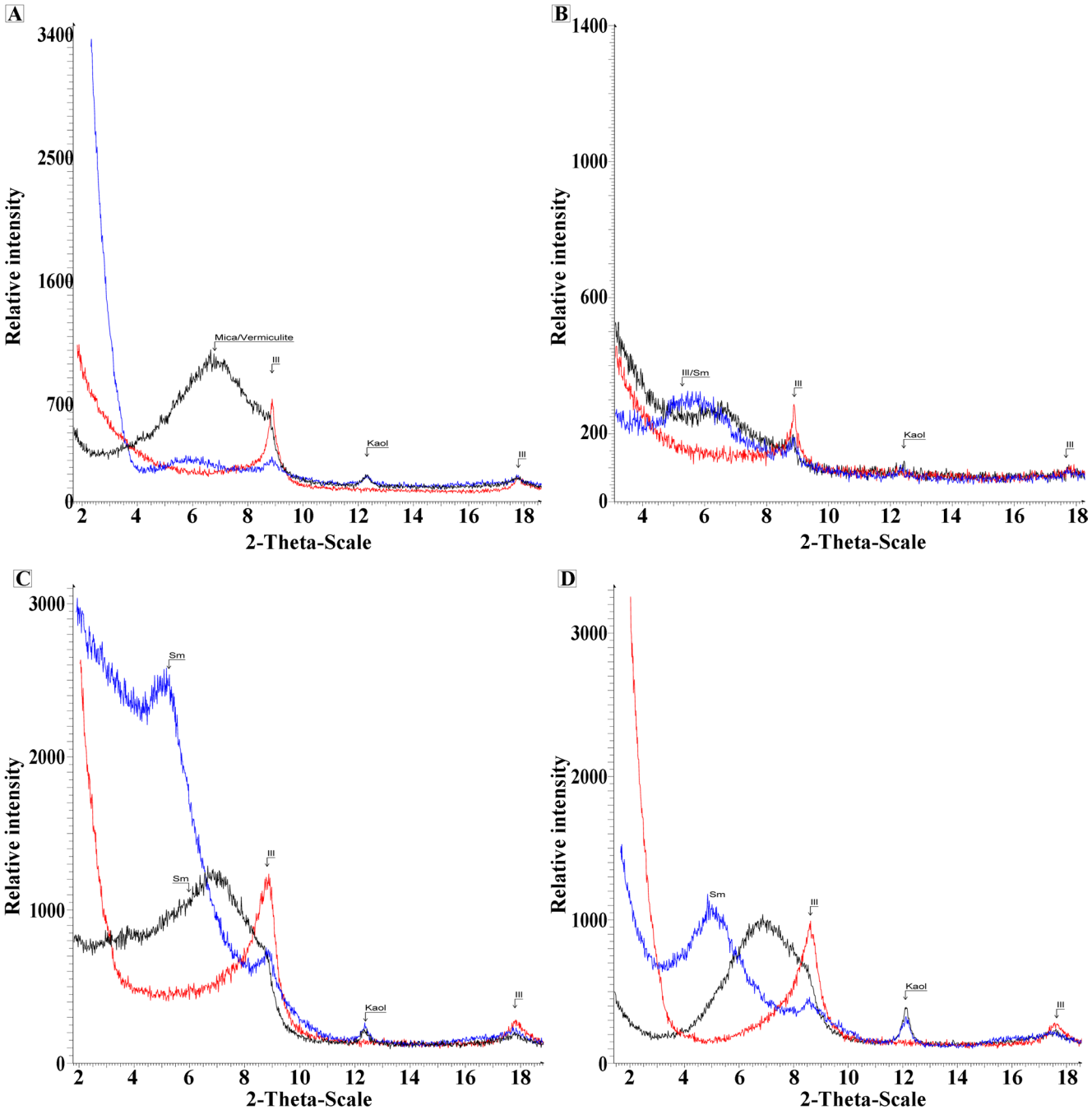

Fig. 9 Representative composite diffractograms of the subgroup identified according to the clay minerals content revealed from the < 2 µm fraction. The black line represents the air dried sample; the blue line represents the ethylene-glycol solvated samples and the red line represents the heated sample at 490 °C. (**A**) Sample TN2b; (**B**) sample TN5a; (**C**) sample TN1b; (**D**) sample TN5b. Abbreviations: Ill = illite; Sm = smectite; Kaol = kaolinite; Ill/Sm = illite/smectite

Discussion

Geochemistry The most significant difference observed among the analyzed samples concerns the amount of calcium relative to all other elements, which display a strong linear correlation with aluminum. This distinction is also evident in the trace element patterns, where samples enriched in SiO_2 and Al-bearing phases tend to show higher concentrations of HFSE and LILE, whereas CaO-rich samples, such as MA1, are generally depleted. The anomalies observed in

both the primitive mantle (PM) and upper continental crust (UCC)-normalized patterns provide further insights into these compositional variations.

Zr and Hf display systematic negative anomalies, which is noteworthy considering that, in clastic sediments, these elements are typically hosted by resistant heavy minerals such as zircon, known for its high stability during weathering, transport and diagenesis. This depletion may result either from a low zircon content in the sediment source or from a dilution effect caused by the high carbonate content of many samples (Carpentier et al. 2009; Garçon et al. 2014; Jones et al. 2017). However, since the anomaly also occurs in the *Bisciaro* samples, where carbonates are less abundant, the persistence of these negative anomalies likely reflects a genuine deficit of zircon-bearing detritus in the sedimentary input.

Similarly, Eu consistently shows negative anomalies, which is typical of sediments derived from felsic crust (Cullers 2000; see also Fig. 7B), where plagioclase fractionation or alteration leads to Eu depletion. This suggests that the Eu anomaly is inherited from the source rocks and is independent of the chosen normalization.

The persistent negative Ce anomaly is a common feature of marine sedimentary environments and is typically associated with redox-controlled fractionation (Tostevin 2020). Under oxic conditions, Ce is selectively removed from seawater by oxidation from Ce^{3+} to the less soluble Ce^{4+}, resulting in its depletion in the dissolved load and, consequently, in the sedimentary record. The systematic negative Ce anomaly recorded in all samples is thus consistent with deposition under oxic marine conditions, in agreement with the known sedimentary setting of the studied formations.

In contrast, the positive Sr anomaly is likely related to its incorporation into the calcite lattice, reflecting the high carbonate content of the analyzed samples.

Another relevant aspect concerns the variable behavior of the samples with respect to the same normalization. For example, the positive Ba anomalies observed in the *Bisciaro* samples — a formation influenced by significant volcaniclastic input — and in a few *Scaglia Cinerea* samples may result from a combination of factors, including the preferential incorporation of Ba into clay minerals or feldspars, or even the precipitation of minor authigenic baryte during early diagenesis (Lash 2015; Scholz et al. 2023). In contrast, the negative Ba anomalies observed in the remaining samples are more easily explained by their higher carbonate content and lower clay mineral fraction, which limits Ba incorporation.

The positive Pb anomaly observed in most samples can be attributed to its association with clay minerals (Lovering 1976; Horowitz 1985). Conversely, the negative anomaly recorded in the archaeological samples and in MA1 is likely due to their lower clay content and the predominance of carbonate phases, which are less effective in retaining Pb.

Therefore, all the observed differences appear to be primarily controlled by variations in the carbonate versus clay mineral ratio, rather than by differences in the provenance of the samples, which all derive from formations deposited in a marine environment.

Mineralogy The predominance of calcite in all samples is fully compatible with deposition in marine pelagic settings, typical of the formations under investigation and the subdivision into three mineralogical groups is mainly controlled by the variable contribution of the detrital siliciclastic fraction (quartz and clay minerals) relative to the carbonate fraction. The most carbonate-rich samples (Group 1) are interpreted as corresponding to intervals of relatively pure carbonate sedimentation, where the detrital input was minimal, resulting in simple mineral assemblages dominated by calcite and quartz. The second group, characterized by a mixture of calcite, quartz and clay minerals, likely represents the most typical situation for these formations, where pelagic carbonate sedimentation was systematically influenced by a moderate input of terrigenous clays. The third group, which includes samples with more diversified mineral assemblages (including opal-CT), could reflect localized variations related either to early diagenetic transformations (such as opal-CT formation from biogenic silica) or to discrete increases in the siliciclastic input, potentially linked to climatic or sea-level variations.

The clay mineralogy, although broadly dominated by smectite and illite, also displays subtle but meaningful variations that further support this interpretation. The observed variability within the *Scaglia Cinerea* samples, for instance, is not easily explained by provenance changes, as all formations have a broadly similar tectono-sedimentary setting. Instead, the differences more likely reflect fluctuations in the carbonate *vs.* siliciclastic supply, combined with variable diagenetic evolution, which may have promoted the formation of mixed-layer phases such as illite/smectite and chlorite/smectite in some samples. Interestingly, the presence of samples with significant amounts of mixed-layer minerals may indicate either more intense burial diagenesis or specific conditions that favored clay mineral transformations. In contrast, samples richer in smectite and poor in mixed-layer clays might reflect less advanced diagenetic stages or an initially smectite-rich detrital input.

Geochemistry *vs.* mineralogy The combined geochemical and mineralogical data provide important insights into the compositional variability and sedimentary processes affecting the analyzed samples. Overall, the variability observed

in the chemical composition closely reflects the mineralogical assemblages identified by XRPD.

The high calcite content detected across most samples is consistent with the widespread presence of carbonate phases. The marked enrichment in CaO correlates directly with the predominance of calcite detected mineralogically, while samples showing lower CaO (*e.g.*, *Bisciaro* Formation and sample TN4a) display a relative enrichment in SiO_2, Al_2O_3, Fe_2O_3, and MgO, which is explained by their higher content of quartz and clay minerals.

The classification of the samples according to Correns (1939, 1949) as ranging from clayey marls to slightly marly limestones is in agreement with both their bulk $CaCO_3$ content and mineralogical composition, confirming that variations in carbonate content dominate the overall rock classification. The clay mineral assemblages further support this subdivision. Samples rich in smectite and illite, particularly within the *Scaglia Cinerea*, correspond to intermediate carbonate contents, while the clay-poor *Maiolica* limestone is mineralogically simple and chemically dominated by CaO.

Scaglia cinerea, *Terra di Nocera* and textile manufacture

In general, the absorbency of a natural clay-rich material is controlled by several factors, including the abundance and type of clay minerals, the specific surface area, the cation exchange capacity (CEC) and the texture of the raw material.

The analyzed samples of *Scaglia Cinerea* show a variable but significant presence of clay minerals, which represent the fundamental component for absorption properties. The clay fraction is dominated by smectite and illite, with subordinate kaolinite and minor amounts of mixed-layer minerals. Among these, smectite is well known for its high swelling capacity, elevated specific surface area and remarkable CEC, all properties that make smectite-bearing rocks highly efficient as natural absorbent materials. Illite, although less expandable than smectite, still contributes to moderate absorptive capacity and, in combination with smectite, may produce a material with balanced properties, suitable both for absorbing liquids and for retaining ions.

Specifically, the *Terra di Nocera* samples (corresponding to TN5a-b in this study) fall within the compositional variability of the *Scaglia Cinerea* formation, showing a clay fraction composed mainly of illite and smectite, with variable but significant carbonate content. Although the presence of carbonate might slightly reduce the overall absorption capacity due to dilution of the clay fraction, the detected clay mineralogy is compatible with a material with useful absorptive properties. The coexistence of smectite and illite suggests that the *Terra di Nocera* could have provided, in antiquity, a readily available, moderately plastic and moderately absorbent material, likely suitable for multiple applications, including medicinal uses, cleaning and treatment of greasy substances or even as pigment extender.

It is also worth noting that, albeit with some variation, the samples from other parts of the *Scaglia Cinerea* formation display similar characteristics. For instance, some levels richer in calcite (*e.g.*, TN2a, TN3a) may have had less favorable absorptive behavior due to the lower relative abundance of clay minerals; conversely, samples such as TN4a, with a more abundant clay fraction, would potentially show improved absorptive capabilities. This suggests that suitable levels for exploitation could be found not only throughout the entire hill where TN5 was sampled but also in other areas within the same formation.

An important aspect is the alteration and pedogenic overprint observed in the *Terra di Nocera* materials (distinguishing *in situ* rocks from the altered loose materials, TN5a *vs.* TN5b). The weathering process likely enhanced the relative clay content by decalcification, improving the physical properties relevant for absorptive applications. This is consistent with the traditional description of *Terra di Nocera* as a white clay or earth.

Finally, it is worth noting that the clay assemblage, dominated by smectite and illite, resembles those of several historical and ethnographically known absorbent clays, such as bentonites or fuller's earth, even though with lower clay contents due to the carbonate dilution. However, as discussed below, it is likely that at least some degree of processing—such as decantation or alkaline treatment—was applied to isolate or enhance the clay fraction, especially when the material was destined for medicinal or cosmetic use. Nevertheless, the combination of availability, sufficient clay content, and presence of smectite would have made the *Terra di Nocera* and possibly selected *Scaglia Cinerea* levels suitable for practical use in ancient contexts.

Creta umbrica, the italic *cretae* and the *cretae* used for textiles

Assuming a correspondence between *creta umbrica* and the *Scaglia Cinerea* used in the production of *Terra di Nocera*, it should be noted that this raw material appears rather unusual when compared to the broader panorama of known *cretae*. However, this impression may also be influenced by the current state of research. In some cases, the main properties of a *creta* can be inferred from ancient textual descriptions with a reasonable degree of plausibility but for many others we lack precise identification and compositional data for comparison are often missing.

For example, among italic *cretae* ancient authors tell us that *Creta Selinusia* dissolved easily in water and that this property made it suitable as a whitewash for plaster, for adulterating *indacum* and as a cosmetic. These characteristics have led some to suggest that it had a calcareous composition, yet we do not know its actual nature or the type of sediment it derived from.

Similarly, in the case of *creta sarda*, it is tempting to suggest that the bentonite deposits were exploited, since they are widely distributed in Sardinia, particularly in association with Oligocene–Miocene calc-alkaline volcanic formations. Their limited whiteness might account for its use in washing rather than in finishing and probably also for the material's modest price, although other economic factors may well have played a role. In this regard, however, it is curious that Pliny does not mention its swelling capacity, which he does highlight for the *saxum* variety, contrasting it with the Sardinian type on qualitative grounds—an omission that invites alternative readings of its composition and mineralogy.

Among the *cretae* explicitly mentioned in ancient sources in connection with textile processing—such as *creta cimolia* and *creta samia*—the former has long been associated with bentonite, based on their local widespread availability (Gliozzo 2007). In the case of *creta samia*, greater uncertainty remains, due to the two different types recorded (*collyrium* and *aster*; see *Nat. Hist*. 35.191). Nonetheless, the availability of bentonites on the island of Samos has led to the suggestion that the aster variety might likewise be identified with this material (Photos-Jones & Hall 2011, pp. 57–61).

In such cases, however, the identification is based on a logical comparison between the reported properties and uses of the *cretae* and the availability of local raw materials, while archaeological evidence is virtually lacking and chemical and/or mineralogical analyses of the raw materials are sporadic at best—entirely lacking in the case of many *cretae*.

Consequently, this raises the question of whether the use of pure bentonite should always be taken for granted. Perhaps we should instead consider a broader range of raw materials that, when suitably processed, could acquire similar properties—particularly in areas like Umbria, where bentonite deposits such as those found in Greece, Turkey or Sardinia are absent.

Another essential point must also be added to all these considerations—namely, the issue of processing. Since we only have access to the raw material, we cannot know what the final product was, either for *creta umbra* or for the ancient *Terra di Nocera*. If its use in textile production may have involved at least manual selection and decantation to isolate a fine fraction richer in clay minerals, its use in cosmetics or medicine likely required a greater number of treatments—not only involving sedimentation or water, or even mixing with other substances but also low-temperature thermal processes. Mixing, for example, with lye (a substance well known to *fullones*), or with natron or even with urine, could have significantly altered the raw material, potentially causing a partial disaggregation of calcareous components, the release of amorphous silica and aluminium with the formation of gels or precipitates and the production of volatile acids through bacterial fermentation, further promoting reactions with carbonates. Each of these processes would have taken the material progressively farther from its original state, making a direct comparison impractical and requiring us instead to focus on assessing the raw material's potential to be transformed into a finished product.

The archaeological samples The archaeological samples show mineralogical and geochemical features broadly comparable to those of the *Scaglia Cinerea*, suggesting that they may indeed derive from similar or even the same geological sources. In particular, sample SC3 displays a composition closely matching that of the *Scaglia Cinerea* sample TN2a, both in terms of carbonate content and clay mineral assemblage. This correspondence supports the hypothesis that SC3 could have originated from the *Scaglia Cinerea* Formation. Conversely, samples SC1 and SC2, although still comparable, show some distinctive features. They are characterized by a higher carbonate content and a slightly lower abundance of clay minerals, which results in a somewhat less favorable absorptive capacity. These differences, however, do not necessarily indicate a different provenance but could instead result from the selection of carbonate-richer levels within the *Scaglia Cinerea* Formation, from post-depositional alteration processes (*e.g*., diagenesis or pedogenesis), or even from an intentional mixing of *Scaglia Cinerea* material with a carbonate-rich source, such as the *Maiolica*. This hypothesis could be supported by the intermediate position of the archaeological samples between the *Scaglia Cinerea* and *Maiolica* samples observed in both the major and trace element diagrams. Nevertheless, the absence of an unquestionable geochemical match calls for caution in drawing definitive conclusions.

Conclusions

This study has contributed to advancing the understanding of the nature, compositional variability and potential applications of *Scaglia Cinerea* and *Terra di Nocera* within their geological and archaeological contexts. By integrating mineralogical and geochemical analyses, we have provided new insights that address key aspects of the research questions.

Firstly, the characterization of *Terra di Nocera* has confirmed its close compositional association with the *Scaglia Cinerea* Formation, of which it could represent the uppermost levels, given the location of the extraction site at the top of the hill. Moreover, the study demonstrates that the *Scaglia Cinerea* Formation contains several levels suitable for the exploitation of clay-rich rocks apart from its outcrop at TN5 hill. In particular, clay-enriched levels (such as TN4a) could have provided materials with even better absorptive properties than those currently known as *Terra di Nocera*. This suggests that the selection of these materials may have extended over a wider area than previously assumed.

Secondly, the presence of significant amounts of illite and smectite, together with a variable carbonate content, supports the hypothesis that these materials were exploited for absorptive applications, such as those historically associated with *creta Cimolia*, used in textile processing, therapeutics and cosmetics. Both *Terra di Nocera* and the *Scaglia Cinerea* display mineralogical and compositional features compatible with the production of moderately plastic and absorbent clays. It is also worth recalling that Pliny distinguished *creta umbrica* from *Cimolia* based on its use, stating that the former was specifically reserved for the refurbishment of garments. This description could be particularly fitting, as the clay minerals provided absorptive capacity, while the high carbonate content contributed to the whitening effect, making it suitable for giving lustre to cloths.

The different marketing practices reported by Pliny—selling *creta umbrica* by volume and *saxum* (likely a bentonite) by weight—are less directly explained but may find a rational interpretation, provided that Pliny was not mistaken. While bentonite is lighter than the *Scaglia Cinerea* at equal volume, its capacity to absorb water significantly increases its weight when wet. In contrast, *Scaglia Cinerea* was likely evaluated based on its dry volume, as its smectite content was insufficient to cause significant swelling, although fine grinding could have enhanced its "fluffy" behavior when dry or mixed with water.

Thirdly, the analysis of the clay loaves from the necropolis of Serravalle di Chienti revealed that the archaeological samples share mineralogical and chemical similarities with the *Scaglia Cinerea* samples, suggesting that the raw material used for their production likely derived from this Formation or nearby units. Although some discrepancies exist—possibly due to natural variability, post-depositional processes, or even intentional selection or mixing of different materials—the data do not indicate the use of geologically unrelated sources. Therefore, while the detected differences prevent drawing a definitive conclusion, the demonstrated compatibility may provide a plausible explanation for the presence of these loaves as grave goods, possibly reflecting the cultural and economic importance of this raw material due to its practical applications.

Indeed, the association of this material with funerary practices—evidenced by its deliberate deposition in tombs and ritual contexts—suggests that its value in antiquity may have extended beyond practical applications. Its presence in burial assemblages, points to a symbolic significance that reflects the esteem in which it was held within the communities that used it.

Lastly, although the analytical results do not constitute direct evidence for unequivocally identifying *Terra di Nocera* with Pliny's *creta umbrica*, they do not contradict this hypothesis; on the contrary, they are fully consistent with it. Much like a case built on converging circumstantial clues, the available findings do not establish identity beyond doubt but strongly support the plausibility of a continuity between the ancient use of the *creta* from Umbria described by Pliny and the Umbrian material known today as *Terra di Nocera*, employed since the 16th century.

Author contributions E.G. wrote the sections "Introduction", "The territory of the Terra di Nocera – geological background", "Materials", "Discussion" and "Conclusions". E.G., V.X. and I.I. jointly wrote the "Methods" and "Results" sections. N.F. authored "The clay loaves in the assemblages of the Umbrian necropoleis". P.L.F. contributed to the geological background and provided financial support for the geochemical analyses. V.X. and I.I. carried out the mineralogical analyses. All authors reviewed and approved the final manuscript.

Funding Open access funding provided by Università degli Studi di Firenze within the CRUI-CARE Agreement.

Data availability All data generated during this study are included in this article.

Declarations

Competing interests The authors declare no competing interests.

References

Bartolucci GB (1636) Sommario sopra le virtù del Bagno dell'Acqua Bianca di Nocera nell'Umbria. Bartoli, Perugia, p 30

Bonomi Ponzi L (1997) *La necropoli plestina di Colfiorito di Foligno*. Ponte San Giovanni (PG): Quattroemme, p. 447
Coccioni R, Montanari A (1994) L'orizzonte del Bisciaro. In: Ciarapica G, Passeri L (Eds). Guide geologiche regionali: Appennino umbro-marchigiano, vol. 7. Lodi (MI): BE-MA editrice, pp. 36–38 (in Italian).
Rudnick RL, Gao S (2014) Composition of the Continental Crust. In: Holland HD, Turekian KK (Eds.) Treat ise on Geochemistry. Oxford: Elsevier, pp. 1–51. https://doi.org/10.1016/B978-0-08-095975-7.00301-6
Bonomi Ponzi L (2014) L'evoluzione del sistema insediativo umbro dalle origini alla conquista romana. In: Camporeale G (Ed). Gli Umbri in età preromana. Atti del XXVII Convegno di Studi Etruschi ed Italici (Perugia, Gubbio, Urbino, 27–31 ottobre 2009). Pisa-Roma: Fabrizio Serra, pp. 189–213.
Broncoli M (2001) Gli ultimi scavi della necropoli di S. Pietro in campo – ex Poligrafico Alterocca Di Terni. Osservazioni preliminari. Ann Mus Faina VIII:343–362
Brumsack H-J (1989) Geochemistry of recent TOC rich sediments from the Gulf of California and the Black Sea. Geol Rundsch 78:851–882
Caldari G (2008) Dai Bagni all'Acqua di Nocera Umbra. Prop Ric 60:115–137
Caley ER, Richards JF (1956) Theophrastus on stones. Ohio State University, Columbus, Ohio, p 238
Camilli A (1627) Del Bagno di Nocera nell'Umbria. Potentissimo á i morsi velenosi, detto acqua Santa, overo acqua Bianca. Trattato utilissimo dove si dichiara la miniera, le virtù, e l'uso di tal'acqua. Angelo Bartoli, Perugia, p 47
Carpentier M, Chauvel C, Maury RC, Mattielli N (2009) The zircon effect as recorded by the chemical and hf isotopic compositions of lesser Antilles forearc sediments. Earth Planet Sci Lett 287:86–99. https://doi.org/10.1016/j.epsl.2009.07.043
Christidis G (1998a) Comparative study of the mobility of major and trace elements during alteration of an andesitic and a rhyolitic rock to bentonite in the islands of Milos and Kimolos, Aegean, Greece. Clays Clay Miner 46:379–399. https://doi.org/10.1346/CCMN.1998.0460403
Christidis G, Scott PW (1997) Origin and colour properties of the white bentonites. A case study from the Aegean Islands of Milos and Kimolos, Greece. Miner Deposita 32:271–279. https://doi.org/10.1007/s001260050092
Christidis GE (1998b) Physical and chemical properties of some bentonite deposits of Kimolos Island, Greece. Appl Clay Sci 13(2):79–98. https://doi.org/10.1016/S0169-1317(98)00023-4
Christidis GE (2001) Formation and growth of smectites in bentonites: a case study from Kimolos Island, Aegean, Greece. Clays Clay Miner 49(3):204–215. https://doi.org/10.1346/CCMN.2001.0490303
Cita MB, Abbate E, Aldighieri B, Balini M, Conti MA, Falorni P, Germani D, Groppelli G, Manetti P, Petti FM (eds) (2005) *Carta Geologica d"Italia 1:50.000. Catalogo delle formazioni – Unità tradizionali (1)*. Quaderni, serie III, vol. 7 (VI). Roma: Servizio Geologico Italiano, p. 318
Correns CW (1939) Die sedimentgesteine. In: Barth TFW, Correns CW, Eskola P (eds) Die entstehung der gesteine. Springer, Berlin, Heidelberg, pp 116–262
Correns CW (1949) Einführung in die mineralogie (Kristallographie und Petrologie). Springer, Heidelberg, Berlin, p 414
Cullers RL (2000) The geochemistry of shales, siltstones and sandstones of Pennsylvanian–Permian age, Colorado, USA: implications for provenance and metamorphic studies. Lithos 51(3):181–203. https://doi.org/10.1016/S0024-4937(99)00063-8
Dalla Fabra L (1712) De Nucerina Terra minerali inter simplicia medicamenta absorbentia ac dulcificantia pro medicinae usu dissertatio. In: Dalla Fabra, L. *Dissertationes physico-medicae.* Ferrariae: Haeredes Bernardini Pomatelli Impr. Episc., pp. 19–45
Frapiccini N (2022) La necropoli plestina di Serravalle di Chienti. Sepolture e rituali funerari. In: Frapiccini N, Naso A (eds) Archeologia Picena. Atti Del convegno internazionale Di studi. Quasar, Roma. Ancona 14/16-11-2019
Garçon M, Chauvel C, France-Lanord C, Limonta M, Garzanti E (2014) Which minerals control the Nd–Hf–Sr–Pb isotopic compositions of river sediments? Chem Geol 364:42–55. https://doi.org/10.1016/j.chemgeo.2013.11.018
Gliozzo E (2007) Supplying Roman Italy with black and white pigments. In: Papi, E. (Ed.) *Supplying Rome and the Empire* (Siena, 2–4 Maggio 2004). Journal of Roman Archaeology. Supplementary Series, 69. University of Michigan Press, pp. 59–71
Guthrie George, Dish David L., Reynolds Robert C. (1995) Modeling the X-ray diffraction pattern of opal-CT. Am Mineral 80(7–8):869–872. https://doi.org/10.2138/am-1995-7-834
Horowitz AJ (1985) *A primer on trace metal sediment chemistry*. U.S. Geological survey Water-Supply Paper, 2277. United States Government Printing Office, Washington, p 67
Jacobilli L (1653) Di Nocera nell'Umbria e sua diocesi e cronologia. Agostino Alterij, Foligno, p 132
Jones III, Piatak JV, Bedinger NM, G.M (2017) Chapter V. Zirconium and hafnium. In: Schulz KJ, DeYoung JH, Seal II, Bradley RR, D.C. (eds) *Critical mineral resources of the united States—Economic and environmental geology and prospects for future Supply*. U.S. Geological survey professional Paper, 1802. Reston. U.S. Department of the Interior. U.S. Geological Survey, Virginia, pp 1–26. DOI: https://doi.org/10.3133/pp1802V
Lash GG (2015) Authigenic barite nodules and carbonate concretions in the upper devonian shale succession of Western New York – a record of variable methane flux during burial. Mar Pet Geol 59:305–319. https://doi.org/10.1016/j.marpetgeo.2014.09.009
Llamazares Martín A (2023) The *Lex Metilia fullonibus dicta* and the production and trade of *Creta Sarda*. Historia 72(2):165–190
Lotti B (1926) Memorie descrittive della Carta Geologica d'Italia. Volume XXI. Descrizione Geologica dell'Umbria. Provveditorato Generale dello Stato, Roma, p 320
Lovering TG (ed) (1976) Lead in the environment. Geological survey professional paper, 957 edn. United States Government Printing Office, Washington, p 90
Morichini D (1807) Saggio medico-chimico Sopra l'acqua Di nocera. Lazzarini, Roma
Ortalli I, Vera A, Antonini A, Bonomi Ponzi L (1986) Mössbauer studies of the Umbria archaeological clays. Hyperfine Interact 29:1133–1136
Pinchi O (1940) Un succedaneo del sapone nelle cave di Bagni di Nocera. *Messaggero (Umbria)* 1 Agosto 1940
Pocobelli GF (2022) Archeologia preventiva e ricerca archeologica: il caso della necropoli di Colfiorito di Foligno (PG). In: Frapiccini N, Naso A (eds) *Archeologia Picena. Atti Del convegno internazionale Di studi* (Ancona 14/16-11-2019), vol II. Quasar, Roma, pp 603–612
Rackham H (1952) Pliny Nat History IX:LibriXXXIII–XXXV Loeb Classical Library, 394. Cambridge, MA: Harvard University Press
Xanthopoulou V, Iliopoulos I (2023) An insight into the suitability of clayey raw materials: the ceramic provinces of the Northern Peloponnese and South Epirus, Greece. Buildings 13(2):473. https://doi.org/10.3390/buildings13020473
Robertson RHS (1949) The fuller's earths of the elder Pliny. Class Rev 63(2):51–52. https://doi.org/10.1017/S0009840X00094749
Sun SS, McDonough WF (1989) Chemical and isotopic systematics of oceanic basalts: implications for mantle composition and processes. In: Saunders AD, Norry, MJ (Eds) Magmatism in the Ocean basins. Geological Society, London, Special Publications,

42. London: Geological Society, pp. 313–345. https://doi.org/10.1144/GSL.SP.1989.042.01.19
Wallinga HT (1996) Official Roman washing and finishing directions - *Lex Metilia Fullonibus Dicta*. Tijdschr Rechtsgesch/Rev Hist Droit/Leg Hist Rev 64(2):183–190. https://doi.org/10.1163/157181996X00166
Robertson RHS (1986) Fuller's earth: a history of calcium montmorillonite. Hythe, Kent, UK: Volturna Press, p 421
Scholz F, Cheng J, Zhang Z, Vosteen P, Siebert C, Frank M (2023) Benthic-pelagic coupling and isotopic fractionation of barium in Kiel Bight, SW Baltic Sea. Front Mar Sci 10:1101095. https://doi.org/10.3389/fmars.2023.1101095
Sigismondi G (1979) La Terra di Nocera. Una ricerca nella storia minore della Scienza. Tipografia Porziuncola, Assisi, p 55
Thorez J (1976) Phyllosilicates and clay minerals. A laboratory handbook for their X-Ray diffraction analysis. Editions G. Lelotte Dison, Belgium, p 579
Tostevin R (2020) *Cerium anomalies and paleoredox*. Elements in geochemical tracers in Earth system science. Cambridge University Press, Cambridge, p 21. https://doi.org/10.1017/9781108847223
Vallocchia F (2000) *Lex Metilia fullonibus dicta*. In: Serrao F (ed) Legge e società nella repubblica romana. vol. 2. Jovene, Napoli, pp 341–378
Vishnia R (1987) *Caius Flaminius* and the *Lex Metilia de fullonibus*. Athenaeum 75:527–534